Marine Geology 352 (2014) 451–468

Contents lists available at ScienceDirect

Marine Geology

journal homepage: www.elsevier.com/locate/margeo

Autonomous Underwater Vehicles (AUVs): Their past, present and future contributions to the advancement of marine geoscience

Russell B. Wynn [a,*], Veerle A.I. Huvenne [a], Timothy P. Le Bas [a], Bramley J. Murton [a], Douglas P. Connelly [a], Brian J. Bett [a], Henry A. Ruhl [a], Kirsty J. Morris [a], Jeffrey Peakall [b], Daniel R. Parsons [c], Esther J. Sumner [d], Stephen E. Darby [e], Robert M. Dorrell [b], James E. Hunt [a]

[a] National Oceanography Centre, European Way, Southampton SO14 3ZH, UK
[b] School of Earth and Environment, University of Leeds, LS2 9JT, UK
[c] Dept of Geography, Environment and Earth Sciences, University of Hull, HU6 7RX, UK
[d] Ocean and Earth Science, University of Southampton, SO14 3ZH, UK
[e] Geography and Environment, University of Southampton, SO17 1BJ, UK

ARTICLE INFO

Article history:
Received 30 July 2013
Received in revised form 9 March 2014
Accepted 14 March 2014
Available online 22 March 2014

Keywords:
Autonomous Underwater Vehicle
AUV
marine geoscience
seafloor mapping

ABSTRACT

Autonomous Underwater Vehicles (AUVs) have a wide range of applications in marine geoscience, and are increasingly being used in the scientific, military, commercial, and policy sectors. Their ability to operate autonomously of a host vessel makes them well suited to exploration of extreme environments, from the world's deepest hydrothermal vents to beneath polar ice sheets. They have revolutionised our ability to image the seafloor, providing higher resolution seafloor mapping data than can be achieved from surface vessels, particularly in deep water. This contribution focuses on the major advances in marine geoscience that have resulted from AUV data. The primary applications are i) submarine volcanism and hydrothermal vent studies, ii) mapping and monitoring of low-temperature fluid escape features and chemosynthetic ecosystems, iii) benthic habitat mapping in shallow- and deep-water environments, and iv) mapping of seafloor morphological features (e.g. bedforms generated beneath ice or sediment-gravity flows). A series of new datasets is presented that highlight the growing versatility of AUVs for marine geoscience studies, including i) multi-frequency acoustic imaging of trawling impacts on deep-water coral mounds, iii) collection of high-resolution seafloor photomosaics at abyssal depths, and iii) velocity measurements of active submarine density flows. Future developments in AUV technology of potential relevance to marine geoscience include new vehicles with enhanced hovering, long endurance, extreme depth, or rapid response capabilities, while development of new sensors will further expand the range of geochemical parameters that can be measured.

1. Introduction

Marine autonomous systems, including submarine gliders and Autonomous Underwater Vehicles, are revolutionising our ability to map and monitor the marine environment (Yoerger et al., 1998, 2007a; Caress et al., 2008; German et al., 2008b). Although truly autonomous systems are typically deployed from a research vessel, they are not tethered to the vessel and do not require direct human control while collecting data (Yoerger et al., 1998; Griffiths, 2003; Yoerger et al., 2007a). They therefore provide opportunities for data acquisition in parts of the ocean previously inaccessible to vessel-based instruments, e.g. beneath ice sheets in polar regions (Bellingham et al., 2000; Brierley et al., 2002; Nicholls et al., 2006; Wadhams et al., 2006; Dowdeswell et al., 2008; Jenkins et al., 2010; Graham et al., 2013), and are improving the spatial and temporal resolutions of a broad spectrum of marine measurements. Marine autonomous systems also have an increasing range of applications in the defence, industry and policy sectors, such as geohazard assessment associated with oil and gas infrastructure (Eddy Lee and George, 2004). In addition, recent economic drivers, such as rapidly increasing vessel fuel oil costs, are making autonomous systems a potentially attractive proposition to organisations responsible for large-scale and cost-effective marine data collection programmes (Wynn et al., 2012).

This contribution will focus on Autonomous Underwater Vehicles, as these platforms are most relevant to geoscience studies that are targeted at or close to the interface between the seabed and the water column. This is a critical interface, as it is a key physical habitat for benthic organisms as well as a zone of focused sediment transport and deposition. The ability to collect high-resolution data from this interface is essential, but technologically challenging (especially in deep water). The aims of this paper are to i) provide an introduction to Autonomous

* Corresponding author.
E-mail address: rbw1@noc.ac.uk (R.B. Wynn).

http://dx.doi.org/10.1016/j.margeo.2014.03.012

Underwater Vehicles and their capabilities, ii) present an overview of their applications in marine geoscience (based upon peer-reviewed scientific literature and new data collected by the authors), and iii) discuss potential future applications and technological advances.

2. Autonomous Underwater Vehicles

Autonomous Underwater Vehicles (AUVs) are unmanned, self-propelled vehicles that are typically deployed from a surface vessel, and can operate independently of that vessel for periods of a few h to several days. Most are torpedo-shaped (e.g. the NERC *Autosub6000* AUV; Fig. 1), but some have a more complex configuration allowing them to move more slowly and across complex terrain, e.g. the WHOI *ABE* and *SENTRY* AUVs (Yoerger et al., 2007a,b). AUVs follow a pre-programmed course and are able to navigate using i) arrays of acoustic beacons on the seafloor (Long Base Line, e.g. Jakuba et al., 2008), or ii) a combination of Ultra Short Base Line acoustic communication, GPS positioning, and inertial navigation (when below the surface — based on dead reckoning using a combination of depth sensors, inertial sensors and Doppler velocity sensors, e.g. McPhail, 2009). Unlike submarine gliders, which are propelled using a buoyancy engine and have an undulating trajectory, AUVs are able to maintain a direct (linear) trajectory through the water and are therefore well suited to geoscience applications requiring constant altitude, such as seabed mapping and subbottom profiling (Mayer, 2006). Remotely Operated Vehicles (ROVs) remain tethered to the host vessel and, while this enables them to draw more power and communicate real-time data, their speed, mobility and spatial range are very limited compared with an AUV. The wholly autonomous nature of some AUVs means that the deploying vessel can be used for other tasks (sometimes geographically separate from the AUV work area) while the AUV is in the water, dramatically increasing the amount of data that can be collected for a given amount of ship-time (Yoerger et al., 2007a,b).

Depending on their pressure resistance, existing AUVs for scientific research can operate in water depths (WD) of up to 6000 m (Fig. 1). The ability of deep-water AUVs to fly relatively close to the seabed (<5 m altitude in areas of low relief) means they are potentially capable of collecting seafloor mapping, profiling and imaging data of far higher spatial resolution (up to two orders of magnitude) and navigational accuracy than surface vessels and towed instruments, which include sidescan sonar (Murton et al., 1992; Scheirer et al., 2000) and camera systems (Jones et al., 2009). AUVs therefore effectively bridge the spatial resolution gap between vessel-mounted or towed systems, e.g. multibeam echosounders (MBESs), sidescan sonars (SSSs) and subbottom profilers (SBPs), and ROV-mounted systems (Fig. 2).

In many cases, AUVs are actually used in conjunction with these systems as part of a 'nested' multi-resolution survey of the seafloor, with i) vessel-mounted MBES or 3D seismic initially providing a regional base map with a spatial resolution of 10s to 100s of metres, ii) AUV MBES providing detailed maps with a spatial resolution of 0.5–5 m, and iii) ROV imaging and sediment sampling subsequently targeting seafloor features as small as a few cm (e.g. Ferrini et al., 2007; Yoerger et al., 2007a,b; German et al., 2008b; Haase et al., 2009; Larroque et al., 2011; Römer et al., 2012; Paull et al., 2013; Fig. 2). For further technical information on AUVs, including their construction, payloads, communications, navigation, power, mission planning, and data processing, see Griffiths (2003), Singh et al. (2004), Kirkwood (2007), Yoerger et al. (2007a,b), Caress et al. (2008), Dowdeswell et al. (2008) and Wynn et al. (2012).

AUVs are capable of carrying a variety of sensor payloads relevant to marine geoscience, including geophysical instruments (MBES, SBP, SSS, magnetometer), geochemical instruments (electrochemical redox sensors), seafloor-imaging tools (high-definition monochrome or colour cameras) and oceanographic instruments (CTD, Acoustic Doppler Current Profilers (ADCPs)). The sensors deployed determine the vehicle altitude, as well as its speed and endurance. Higher power sensors, e.g. SSS and SBP, reduce endurance due to their increased energy requirements, while high-resolution seafloor imaging with a colour camera system will require the AUV to fly slower and closer to the seabed than if it was undertaking a MBES survey (Yoerger et al., 2007a). The ability of AUVs to continuously collect large volumes of data during multiple missions also introduces new challenges in terms of data analysis and storage (e.g. Jerosch et al., 2006; Caress et al., 2008; Williams et al., 2010; Lucieer et al., 2013).

AUVs cannot operate everywhere, and certain factors need to be taken into account during mission planning (Wynn et al., 2012). AUVs used in marine geoscience typically move at speeds of up to 1.5–2.0 m/s^{-1}, and can be influenced by tidal (or other) currents approaching or exceeding these velocities (negative impacts include 'crabbing' of the vehicle and navigational drift, both of which can significantly affect data quality). AUVs may also be less well suited for deployment in areas of high military, shipping or fishing activity, due to

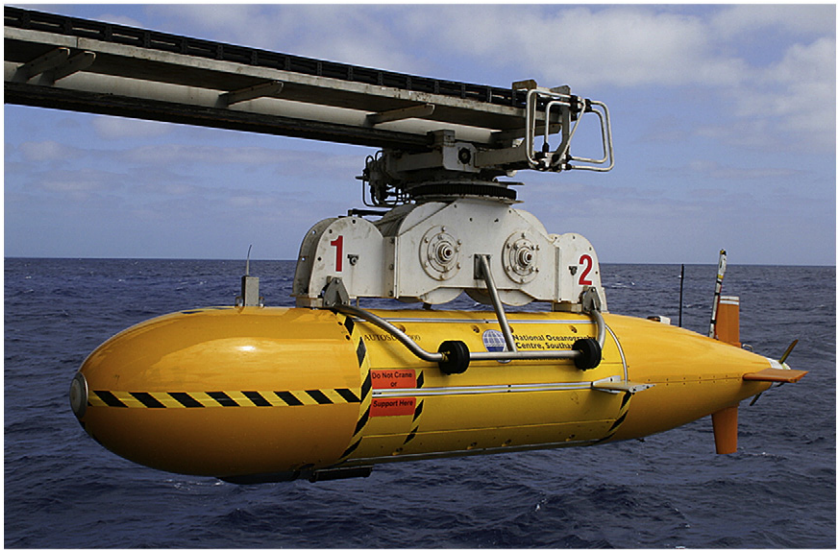

Fig. 1. The UK Natural Environment Council (NERC) *Autosub6000* AUV, depth-rated to 6000 m, can be equipped with multiple payloads for marine geoscience research, including a high-resolution multibeam echosounder, sub-bottom profiler and sidescan sonar, a colour camera system, and Conductivity, Temperature, Depth (CTD) and electrochemical redox (Eh) sensors. The vehicle is 5.5 m long and has a dry weight of 1800 kg; it is capable of precision navigation and terrain following, and has a sophisticated collision avoidance system.

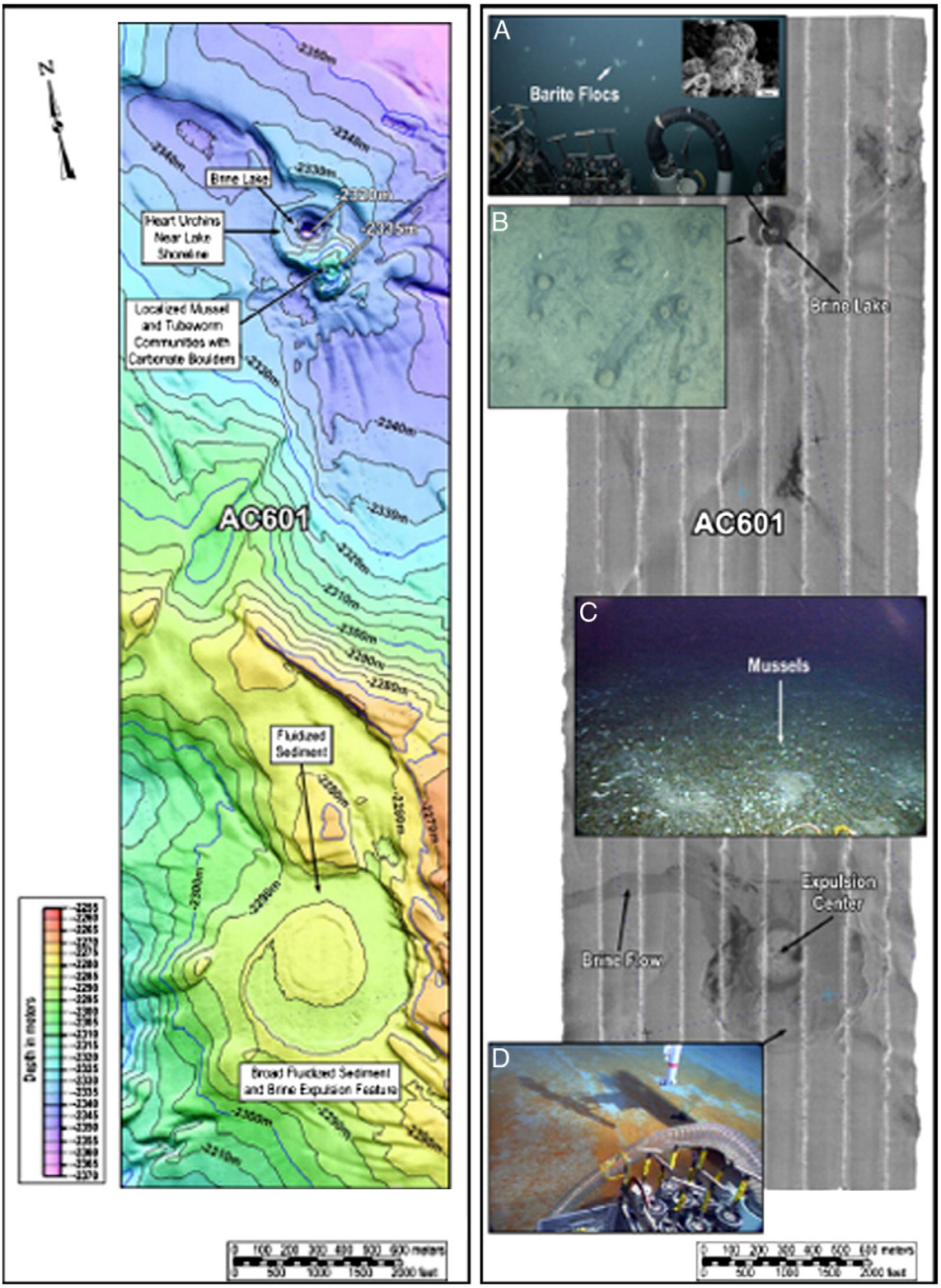

Fig. 2. High-resolution AUV MBES bathymetry (left) and backscatter mapping (right) of cold-seep features in the deep-water northern Gulf of Mexico. Sites for detailed AUV mapping were selected through analysis of shipborne 3D seismic surface amplitude and bathymetry data. Subsequent ROV dives targeted specific features of interest on the AUV maps; these ROV images revealed that the brine lake in the north of the area hosted floating flocs of barite (A) and abundant heart urchins around the lake margins (B), while zones of abundant mussels (C) corresponded to zones of elevated backscatter (dark tones) in the fluid expulsion centre to the south. The latter site was also sampled (D) to investigate orange-stained muds visible at the seafloor. This study illustrates the power of a nested survey approach, with AUVs bridging the resolution gap between shipborne 3D seismic and ROV data.
From Roberts et al. (2010).

acoustic interference, collision risk, and net entanglement. Areas of high water-column turbidity, e.g. phytoplankton blooms or areas of high fluvial run-off, may hinder camera-based seafloor imaging. Although relatively 'quiet' compared to research vessels, AUVs may disturb marine fauna in sensitive regions, e.g. Marine Protected Areas, especially when running acoustically loud geophysical sensors. Although many

of these external factors also affect research vessels, AUVs are generally less well suited to tidally dominated shallow-water settings that have high levels of anthropogenic infrastructure and activity.

3. AUV applications in marine geoscience

AUVs have been deployed in a wide variety of marine geoscience studies, originally focused on seafloor mapping but more recently expanding into water column geochemical and oceanographic measurements. The first AUV specifically deployed for marine geoscience was probably the IFREMER *L'Epaulard* AUV, which was used in the early 1980s to map deep-sea manganese nodule fields (Galerne, 1983). By the early 1990s, over 56 different AUVs were described in the published literature, although almost all were demonstration vehicles that were unproven in the field (Bellingham and Rajan, 2007). However, by 2007, a total of 92 *REMUS* AUVs alone were being used in the field, of which 82 were for military use and the remaining ten for scientific purposes (Moline et al., 2007). The increased use of AUVs in the marine environment is mirrored in peer-reviewed marine geoscience publications featuring AUV datasets (Fig. 3). This upsurge is also reflected in the amount of information now available on the global internet, e.g. Google searches undertaken in July 2013 for *AUV marine geoscience* and *Autonomous Underwater Vehicle marine geoscience* returned ~300,000 and ~1,050,000 individual hits, respectively.

Examples of AUVs that have been used extensively for marine geoscience include the 6000 m-depth-rated NERC *Autosub6000* (McPhail, 2009; Fig. 1), the 6000 m-depth-rated MBARI *D. Allan B.* (Kirkwood, 2007; Caress et al., 2008), the 6000 m-depth-rated WHOI Autonomous Benthic Explorer *ABE* (Yoerger et al., 2007a,b), the 5000 m-depth-rated MARUM *Seal 5000* (Römer et al., 2012; Marcon et al., 2013), the 6000 m-depth rated IFM-GEOMAR *ABYSS* (Haase et al., 2009), the 3000 m-depth-rated Ifremer *AsterX* (Dupré et al., 2008), the 3500 m-depth-rated JAMSTEC AUV *Urashima* (Kumagai et al., 2010; Nakamura et al., 2013) and the 700 m-depth-rated ACFR AUV *Sirius* (Williams et al., 2010; Lucieer et al., 2013). A number of other AUVs have come into recent service in the science sector, and join a growing number of established providers in the commercial sector, e.g. Kongsberg *REMUS* and *Hugin*.

The broad scientific categories of AUV use up to the present day are discussed below.

3.1. Submarine volcanism and hydrothermal vents

One of the commonest applications of AUVs in marine geoscience, as represented in peer-reviewed scientific literature, relates to the study of submarine volcanism and hydrothermal vents. In this setting, AUVs can be used to i) make high-resolution bathymetric and magnetic field maps of the seafloor, ii) locate active hydrothermal plumes, using a combination of temperature, optical backscatter, electrochemical redox (Eh), vertical velocity and SSS imagery, and iii) produce detailed geo-referenced photomosaics of specific areas of interest (e.g. Yoerger et al., 2007a; German et al., 2008b; Nakamura et al., 2013).

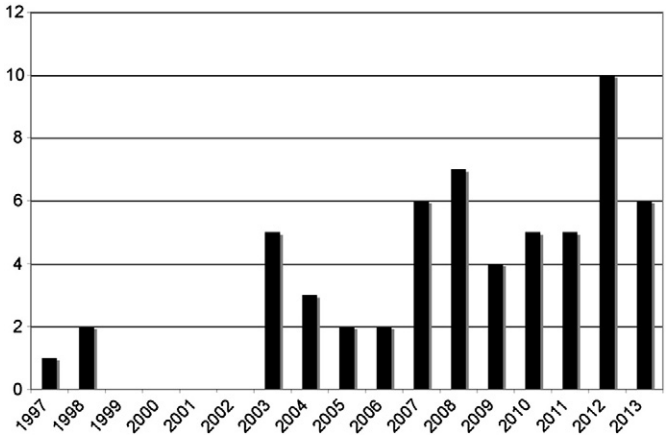

Fig. 3. Graph showing annual totals of peer-reviewed papers featuring new marine geoscience data collected using AUVs. Note the rapid upsurge in the last ten years. All papers featured in the graph are included in the references.

Some of the first marine geoscience publications utilising AUV data involved the WHOI AUV *ABE*, following its deployment over the Juan de Fuca Ridge, off northwest USA, in 1995 and 1996 (Tivey et al., 1997, 1998; Yoerger et al., 1998). The primary aim was to survey a young (two years old) lava flow at 2200 m WD using a magnetometer; the results demonstrated the value of high-resolution magnetic data for detecting and mapping new lava flows. The vehicle also imaged the seafloor with a video system and used CTD data to map a hydrothermal plume. A series of pioneering studies subsequently used high-resolution bathymetric and magnetic mapping data, collected with *ABE*, to investigate mid-ocean ridge crest environments on the East Pacific Rise (Carbotte et al., 2003; Cormier et al., 2003; Shah et al., 2003; Fornari et al., 2004; Ferrini et al., 2007). These data were used to identify a number of processes, including i) magmatic subsidence, as revealed through fault restoration of ridge crest bathymetry (Carbotte et al., 2003), ii) episodic dike swarms, using magnetic field data (Shah et al., 2003), iii) contrasting eruptive styles, representing waxing and waning volcanism on millennial time scales (Cormier et al., 2003), and iv) spatial relationships between hydrothermal vents and primary volcanic features and processes (Fornari et al., 2004; Ferrini et al., 2007).

On the Mid-Atlantic Ridge (MAR), *ABE* was used to map the spectacular Lost City hydrothermal vent field at 750–900 m WD (Kelley et al., 2005). The high-resolution MBES data obtained with the AUV, in conjunction with video and sample data obtained from a ROV (DSV *Alvin*), allowed the relationships between faulting and active venting at this topographically complex site to be explored in detail. *ABE* also surveyed the slow spreading southern MAR to identify sites of active hydrothermal venting (German et al., 2008a). As well as identifying evidence for recent volcanic eruptive activity, the surveyed vents were shown to be emitting fluids at over 400 °C, making them the hottest vent fluids reported at the time from a ridge crest setting. Elsewhere, *ABE*, and its successor, *SENTRY*, have been used to investigate hydrothermal venting on Galapagos Rift (Shank et al., 2003), Southern Explorer Ridge in the northeast Pacific (Deschamps et al., 2007) and Brothers Volcano, New Zealand (Baker et al., 2012; Caratori Tontini et al., 2012; Embley et al., 2012).

ABE was typically deployed as part of a three-phase 'nested' survey strategy, involving vessel, AUV and ROV, e.g. Yoerger et al. (2007a,b) and German et al. (2008b). This three-phase strategy was also used successfully in the recent discovery of the deepest hydrothermal vent system known on Earth, using the NERC *Autosub6000* AUV (Connelly et al., 2010). In early 2010, the RRS *James Cook* surveyed an area of about 1000 km^2 of the Cayman Trough, a 100 km-wide rift basin within the central Caribbean Sea that is bound to the north and south by two major fault systems up to 7000 m deep. Shipborne MBES (Simrad EM120) and deep-towed TOBI 30 kHz SSS mapping were used to establish a broad-scale base map of the Mid-Cayman Spreading Centre (MCSC) (Fig. 4A), which revealed a series of interesting targets for subsequent AUV mapping. The first AUV mission was therefore a terrain-following survey of the 5000 m-deep seafloor, with high-resolution MBES (EM2000) used to map the seabed at an altitude of 75 m, and optical and electrochemical sensors (nephelometry and Eh) used to map particulate and reduced iron plumes in the near-bottom water column. This initial survey occupied track lines that were spaced 100 m apart and 1 km long, with a combined track length of 65 km over the 24-hour mission. The AUV data obtained during this initial mission were highly indicative of chemically reduced effluent being produced from a series of mounds on the seafloor, subsequently referred to as the Beebe Vent Field (Fig. 4B–C). These data guided subsequent missions with the NERC ROV *Isis*, which was able to navigate the rugged terrain and evade vent fluids emitting at >400 °C.

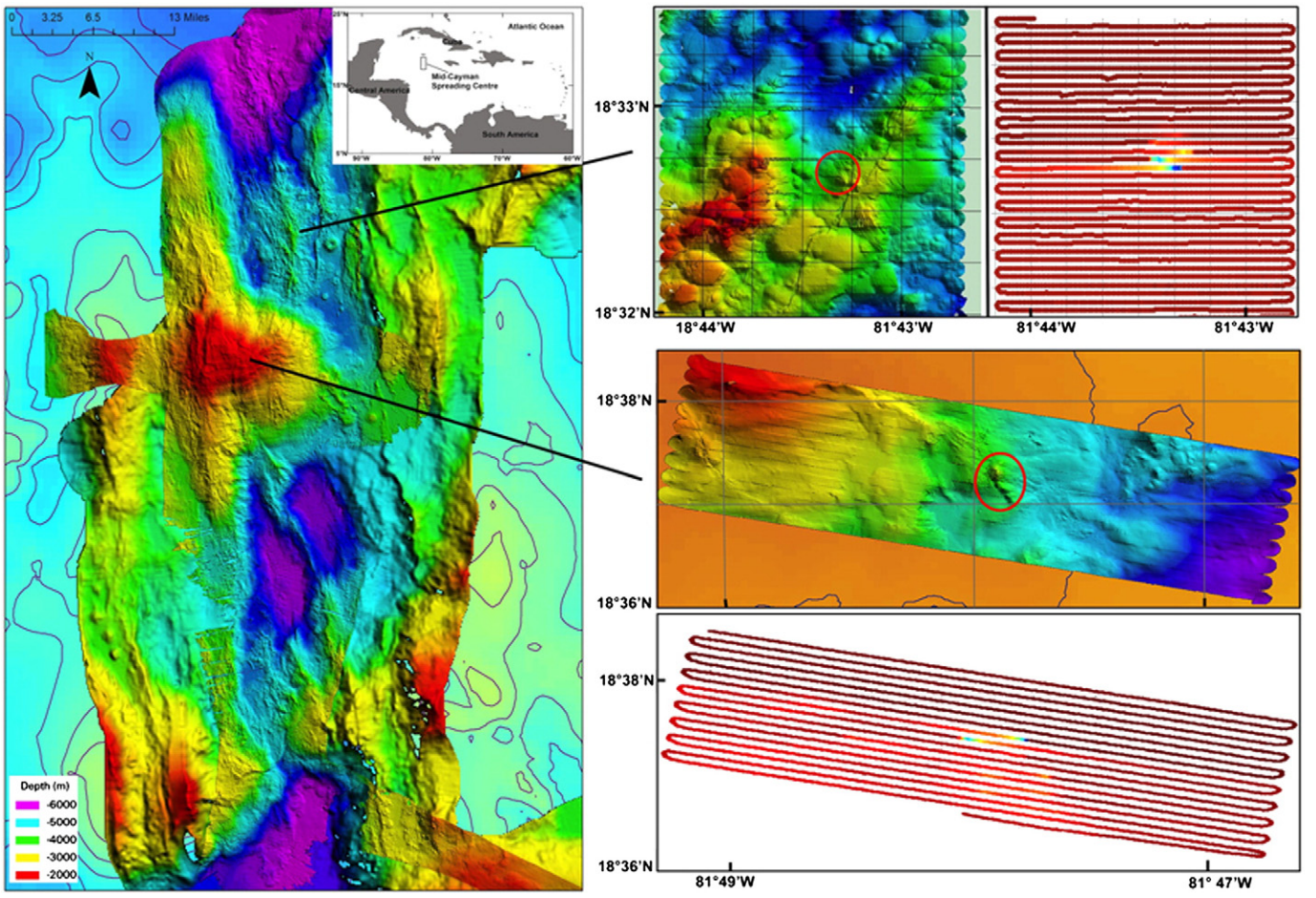

Fig. 4. (A) Shipborne MBES map of the Mid-Cayman Spreading Centre, superimposed on a background of regional GEBCO bathymetry, showing the general structure of the rift. Inset map shows location of the Mid-Cayman Spreading Centre relative to Central America and the Caribbean archipelago. (B) EM200 (1 m resolution) MBES derived from *Autosub6000* showing a NE–SW alignment of volcanic domes (each ranging between 200 and 600 m in diameter); the red circle indicates the position of the Beebe Vent Field at 5000 m WD (legend: red = 4760 m, dark blue = 5260 m). (C) Signal strength from an Eh sensor on *Autosub6000* (legend: blue = low Eh, red = high Eh) acquired at the same time as the EM200 MBES; the negative Eh signal is indicative of reduced fluids entering the water column from an active hydrothermal source located on the seafloor. (D) EM200 (1 m resolution) MBES derived from *Autosub6000* showing a series of cones (of between 50 and 130 m in diameter and 60 m high); the red circle indicates the position of the Von Damm Vent Field at 2200 m WD (legend: red = 2000 m, purple = 2800 m). (E) Signal strength from the Eh sensor on *Autosub6000* (legend: blue = negative Eh, red = positive Eh) showing a pattern of low Eh in the location of the Von Damm Vent Field. Dispersed low Eh signals to the south of the main cone indicate diffuse emissions of reduced vent fluid from a broad area.

The ROV was used for close-up photography, sampling, and placement of experiments and sensors on the active vent structures (Connelly et al., 2010).

The second AUV mission took place at ~2500 m WD on the western flank of the MCSC, and covered an area of 1.5 × 3.0 km in 28 h with a track line spacing of 75 m. A number of distinct Eh signals were detected over the summit of a conical-shaped mound, which is 130 m in diameter and 50 m high (Fig. 4D–E). The unusual shape of the mound and its association with strong Eh signals indicated that it was a site of active hydrothermal fluid emission, subsequently termed the Von Damm Vent Field. With the target site located, the ROV was again deployed to investigate visually, and sample the substratum and fauna. As a result, the conical mound was confirmed as a site of voluminous hydrothermal fluid emissions and host to abundant vent-specific fauna (Connelly et al., 2010). Overall, these data highlight the benefits of using a nested multi-resolution survey approach, for efficient discovery and characterisation of active hydrothermal vent sites in the deep ocean.

Further important discoveries in submarine volcanic settings have recently been made using other deep-water AUVs. For example, Marcon et al. (2013) used the MARUM *Seal 5000* AUV to map the Menez Gwen hydrothermal vents, which, at 800 m WD, are the shallowest known vents on the MAR that host chemosynthetic communities. Kumagai et al. (2010) used the JAMSTEC *Urashima* AUV to map the Iheya–North hydrothermal vent field off Okinawa. In addition to high-resolution bathymetric and backscatter mapping of the seafloor, novel application of AUV SSS imagery enabled detection of active hydrothermal plumes in the water column with upwelling speeds of ~1 m/s. The presence of active plumes was confirmed by CTD and pH sensor data derived from the AUV. Yoshikawa et al. (2012) then used *Urashima* to undertake the first detailed morphological study of hydrothermal systems in the Mariana Trough. Nakamura et al. (2013) subsequently focused on AUV mapping data from a 5 × 5 km area across one of these Mariana Trough sites, the Pika hydrothermal vent site. A new hydrothermal vent site (named *Urashima*, after the AUV) was inferred to be adjacent to the Pika site based on AUV magnetisation and MBES data, and active venting into the water column at this location was imaged using 120 kHz SSS data (Fig. 5) and confirmed with ROV imaging. These recent studies using *Urashima* highlight the ability of AUVs not only to map existing and discover new hydrothermal vent sites, but also to confirm active venting at the seafloor using SSS imagery. This more direct method overcomes some of the problems associated with geochemical mapping of diffuse hydrothermal plumes, e.g. dispersal by deep bottom currents (German et al., 2008b), and aids identification of closely spaced vent sites.

Finally, Clague et al. (2011) used the MBARI *D. Allan B.* AUV to investigate volcanic processes and products of West Mata Volcano in the northern Lau Basin. High-resolution AUV bathymetry data were used to image the fine-scale morphology of the volcano's eruptive vents

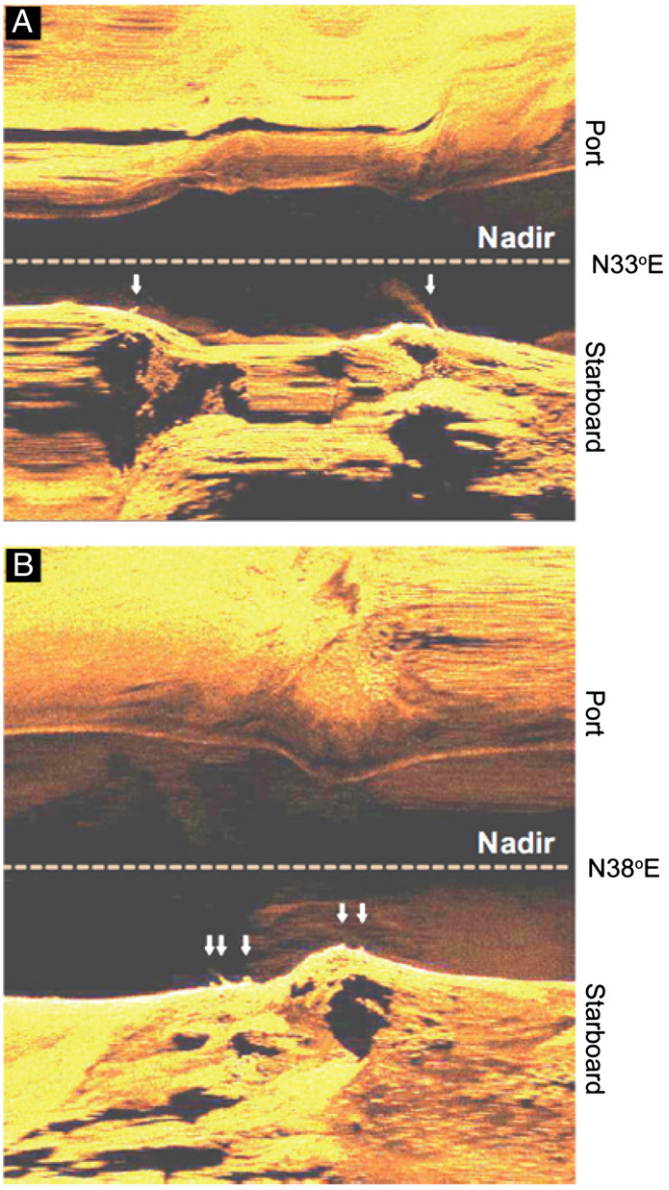

Fig. 5. Unprocessed SSS images obtained (A) above the Pika hydrothermal vent site, and (B) 500 m north of the Pika site. The black area in the central part of each image represents the water column. White arrows show the loci of presumed hydrothermal plumes discharging into the water column.
From Nakamura et al. (2013).

and rift zones. Although the AUV was flown at 75 m above seabed over the entire rift system and summit area, acoustic noise on the subbottom chirp profiler was only recorded over a small area of the summit (near the Hades and Prometheus vents). This noise was interpreted to represent eruptions at these vent sites, and confirmed earlier observations indicating that recent activity was confined to the summit area. The AUV mapping data will aid more accurate calculation of volume changes if the eruption continues and if a repeat mapping survey is conducted in the future. The importance of repeat AUV mapping to understand volcanic processes was subsequently illustrated by Caress et al. (2012), who again used the *D. Allan B.* to generate the first high-resolution maps of lava flows from a single eruptive event on an active underwater volcano. The AUV initially collected one-metre-resolution multibeam bathymetry maps across the summit of Axial Seamount at 1300–2400 m WD during 13 surveys in 2006–09 (e.g. Thomas et al., 2006), with the aim of mapping eruptive products of the historical 1998 eruption. A further eruption in 2011 provided an opportunity to undertake repeat mapping with the same AUV, thereby allowing the spatial extent, thickness and morphology of new lava flows to be detected. Mapping data were subsequently ground-truthed with ROV video and samples. The ability to map individual flows provided new insights into flow behaviour, including indicators for both high and low eruption rates during the same event, reactivation of pre-existing fissures, and reoccupation of pre-existing channels. The reoccupation of pre-existing flow channels highlights the difficulty of mapping products of individual eruptive events without high-quality 'before-and-after' bathymetric surveys.

3.2. Fluid-escape features and chemosynthetic ecosystems

As well as mapping and monitoring of deep-water hydrothermal processes, AUVs have played an important role in investigating low-temperature fluid escape features. Paull et al. (2008) used the MBARI *D. Allan B.* AUV to collect high-resolution MBES (lateral resolution 1.5 m), SBP (0.1 m vertical resolution) and SSS data over a series of fluid escape mounds and surrounding swells at 800–900 m WD in Santa Monica Basin, offshore California. These mapping data provided broader geological context for detailed ROV sampling, while SBP profiles provided indications for small-scale active faulting extending to the seafloor (supported by ROV data showing elevated methane concentrations, chemosynthetic fauna and seafloor alteration in these areas). The high-resolution AUV data contributed to the interpretation that the features are 'blisters' formed by expansion associated with gas hydrate accumulation in the subsurface; this interpretation supported the 'submarine pingo' hypothesis previously developed by Hovland and Svensen (2006) for seafloor blisters on the Norwegian margin. Newman et al. (2008) used the WHOI *SeaBED* AUV to investigate a series of giant km-scale seafloor pockmarks along the shelf edge (~100 m WD) off the east coast of the US. The AUV flew at an altitude of ~3 m, and was carrying a methane sensor to measure in situ dissolved methane concentrations across the pockmarks. High-resolution MBES, CTD and colour photography data (44,000 images) were also collected with the AUV. The results indicated that active methane venting is occurring at present and is focused along pockmark walls, and provided new information on spatial and temporal variations in methane concentrations.

In the Mediterranean, Dupré et al. (2008) used the Ifremer *AsterX* AUV to map two active mud volcanoes on the eastern Nile Fan, offshore Egypt, at 1–2 m horizontal resolution. The high-resolution AUV mapping data revealed numerous features that were unresolvable on ship-mounted MBES data, and provided new insights into the formation and evolution of the mud volcanoes, Amon and Isis, which are at water depths of 1120 and 990 m, respectively (Foucher et al., 2009). Fluid escape was focused at the centres of the mud volcanoes, leading to a high density of seeps, expulsion of mud breccia blocks, deformation of the mud volcano surface, and small landslides at the margins of the mud volcanoes. The authors also acknowledged the potential for repeat mapping in the future, to monitor seabed deformation associated with mud volcano growth. Moss et al. (2012) used a hydrocarbon industry AUV dataset, comprising 6750 line-km of chirp SBP and MBES bathymetry and backscatter, to map >25,300 pockmarks across a ~1000 km^2 area of the Rosetta Channel region of the Nile Fan. The majority of pockmarks were at 400–800 m WD, and the high-resolution mapping data allowed spatial statistics relating to pockmark distribution and density to be applied. Highest densities were >600 pockmarks/km^2, and the AUV data allowed a new conceptual model for pockmark distribution to be developed (termed the 'pockmark drainage cell').

In the Black Sea, Römer et al. (2012) used the MARUM *Seal 5000* AUV to generate high-resolution MBES maps of fluid escape features in the Kerch seep area at 890 m WD. AUV mapping provided evidence for active mound formation and associated faulting and gravitational mass movements; subsequent ROV dives confirmed active methane venting. The discovery of low-relief mounds (<10 m high) and associated active venting is important in determining regional and global methane flux

budgets, as previous work on deep-water seepage in the Black Sea was only focused on conspicuous mud volcanoes.

A number of recent papers have taken advantage of hydrocarbon industry AUV data to investigate active fluid flow processes in the Gulf of Mexico. Roberts et al. (2010) used hydrocarbon industry 3D seismic, ROV and AUV data (MBES, SSS and SBP) to investigate fluid escape processes at four cold seep sites in the deep-water Gulf of Mexico at 1050–2340 m WD (Fig. 2). AUV data provided new insights into formative processes of i) highly saline and methane-enriched brine lakes, ii) active methane-emitting mounds with thriving chemosynthetic communities, and iii) a large ridge with cold-seep carbonate blocks and extensive deep-water coral communities. AUV data were also used to plan subsequent ROV dives for ground-truthing and sampling purposes (Fig. 2). This study provided the first comprehensive understanding of cold seep processes from the northern Gulf of Mexico at >1000 m WD, and the interplay between geological and biological responses at these seepage sites. Macelloni et al. (2012) integrated 3D seismic data with a very high-resolution AUV 2D chirp SBP dataset, to investigate shallow hydrocarbon fluid flow associated with the Woolsey Mound in the northern Gulf of Mexico. The profiler data were collected with a C&C technology *Hugin 3000* AUV, at 900 m WD. The AUV data provided new insights into active processes, for example a fault imaged on 3D seismic data that appeared to terminate in the sub-surface, was shown on 2D AUV profiles to actually propagate through to the surface (Fig. 6); this fault corresponded with a seafloor pockmark imaged on MBES data and provided an obvious target for subsequent monitoring of hydrocarbon leakage.

Finally, Wagner et al. (2013) used the WHOI *SENTRY* AUV to investigate geochemical–biological interactions at cold seep communities associated with the Blake Ridge Diapir off South Carolina, eastern USA (Fig. 7). The AUV collected MBES, SSS and digital photo data across a series of seafloor pockmarks covering 0.131 km^2, with the photo dataset comprising 5568 georeferenced images that were used to classify faunal characteristics. Several new seep communities were discovered using the new high-resolution data, and the observed concentric zonations of mussels and clams around the pockmarks provided useful insights into the influence of chemical gradients on megafaunal distribution (Fig. 7).

3.3. Benthic habitat mapping

AUV data have also been applied to benthic habitat mapping studies at a range of water depths, including very shallow coastal environments. For example, Moline et al. (2007) used a *REMUS* AUV to map benthic eelgrass habitats in the Strait of Juan de Fuca, northern USA, in water depths as shallow as 1–2 m (one survey line was aborted due to eelgrass being caught in the AUV propeller!). Multi-spectral radiometers were used to delineate benthic habitats (including eelgrass), and were ground-truthed with underwater video data. Kennish et al. (2004) also used a *REMUS* AUV, equipped with high frequency (600 kHz) sidescan sonar and ADCP, to undertake benthic habitat mapping in the estuarine environment of Great Bay, New Jersey. The AUV surveyed a strip of seabed covering 0.2 × 1.1 km in very shallow water depths (0.5–10.5 m at mean low tide), in an area with tidal currents exceeding 2 m/s. Sidescan sonar mapping provided information on a variety of tidally generated bedforms (ripples, dunes and sand waves), with wavelengths and heights as low as 0.1 m; accompanying grab samples provided important ground-truthing of sediment character. These studies successfully demonstrate that AUVs can provide valuable data on seafloor habitats in dynamic shallow-water environments. Other shallow-water habitat mapping studies, using AUV derived seafloor images, have investigated coral communities off Puerto Rico (Singh et al., 2004), the US Virgin Islands (Armstrong et al., 2006), the Great Barrier Reef in Queensland, Australia (Williams et al., 2010) and the Tasman Peninsula, Tasmania (Lucieer et al., 2013).

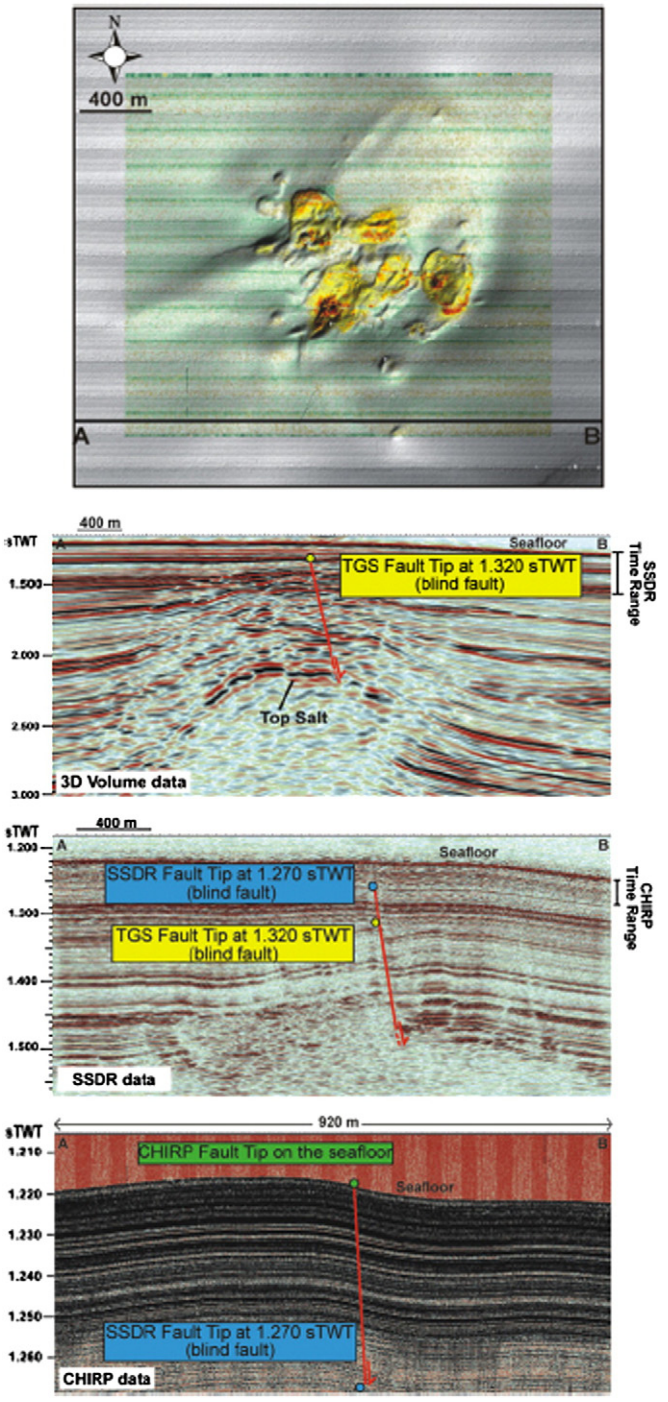

Fig. 6. Map view (top) and 2D profiles (below) of a fault adjacent to the Woolsey Mound at 900 m WD in the Gulf of Mexico. Integration of multiple-resolution datasets has been key to imaging fault displacement and the active tectonic regime. Comparison of one particular fault across the three datasets, mapped on a line located in the southern portion of the mound, has shown that the fault, which appears to terminate at 1.30 s TWT in the 3D volume, continues up to 1.240 s TWT in the SSDR and actually reaches the seafloor based on the AUV chirp data.
From Macelloni et al. (2012).

New data, collected with the NERC *Autosub6000* AUV in July 2102, highlight the potential for AUVs to undertake Marine Protected Area (MPA) mapping and monitoring in open shelf environments. *Autosub6000* was deployed in the Greater Haig Fras area of the UK continental shelf from RRS *Discovery* cruise 377 (Ruhl et al., 2013). Haig Fras is an isolated, bedrock outcrop some 90 km north west of the Isles of Scilly at ~100 m WD. It is thought to be the only substantial area of

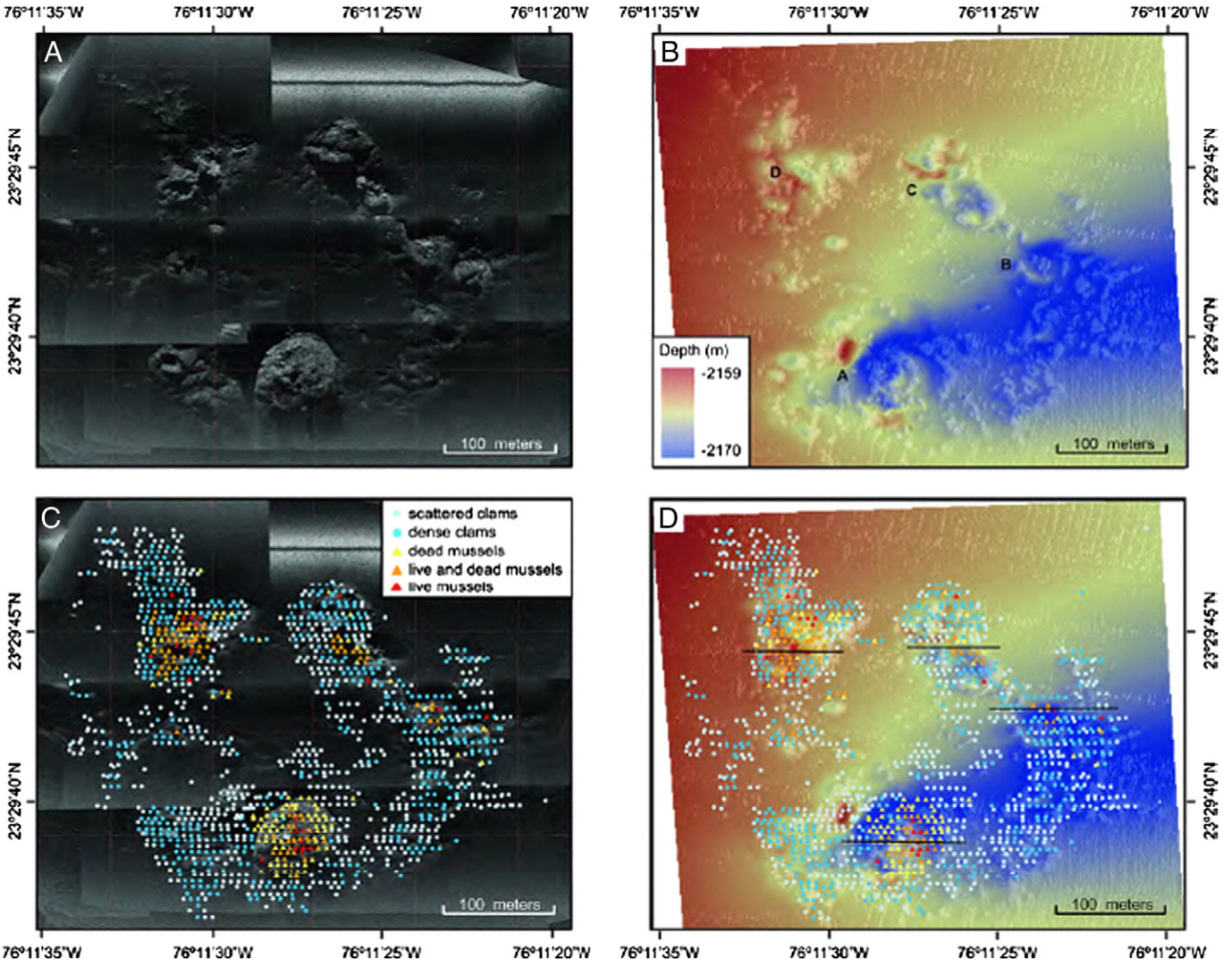

Fig. 7. AUV SSS and MBES data, and faunal distribution maps, across a series of pockmarks at the Blake Ridge Diapir site. (A) AUV SSS data (2 m horizontal resolution), light tones = high backscatter and dark tones = low backscatter; (B) AUV MBES data (1 m horizontal resolution), showing the four pockmarks (A–D); (C) seep megafaunal distributions overlain on the AUV SSS data; (D) seep megafauna distributions overlain on the AUV MBES data.
From Wagner et al. (2013).

rocky reef in the Celtic Sea beyond the coastal margin. The rock outcrop is the focus of both a Special Area of Conservation and a proposed Marine Protected Area (JNCC, 2008). The purpose of this deployment was to i) obtain data on the nature of the seabed environment and its fauna, ii) serve as a comparator with a similar survey carried out from a surface vessel (*RV Cefas Endeavour*; Coggan, 2012), and iii) provide a baseline dataset for future monitoring in order to assess whether protection measures are effective.

The AUV deployment consisted of three survey dives, the vehicle surfacing between each dive to refresh its GPS position. The first dive was to undertake a MBES survey (with the vehicle at 50 m altitude), the second was a photographic survey (3 m altitude) and the third was a SSS survey (15 m altitude). The primary survey instrumentation was: (i) EM2000 MBES system; (ii) EdgeTech 2200-FS dual frequency SSS (120/410 kHz); and (iii) Point Grey Research Grasshopper 2 digital camera GS2-GE-50S5C (Sony ICX625AQ sensor) with 10 J flashgun. Full details of the mission and vehicle set-up are in Wynn et al. (2012).

Fig. 8A provides a comparison of *RV Cefas Endeavour* and *Autosub6000* MBES data. In terms of both topographic interpretation and georeferencing, the two datasets are highly consistent. The ship's MBES backscatter and AUV SSS seabed fabric interpretation and georeferencing were also very similar (Fig. 8B). Some 15,000 seabed images were recorded during the photographic survey. They were somewhat degraded by particle backscatter in the near-bottom water, but of sufficient quality for seabed characterisation and the general identification of megabenthos and demersal fish. For rapid seabed classification only every 30th frame was categorised: (i) bed rock; (ii) boulder; (iii) coarse (mixed sediment); (iv) 'mega-ripples' (sediment waves, metre-scale wavelength, decimetre amplitude); and (v) fine rippled (sands and muddy sands) (Fig. 8E–H). As a biological marker for 'good reef habitat', the occurrence of abundant Zoanthidea (colonial anemones) was also recorded (Fig. 8D). There was a close match between the photographic classification and variations in acoustic fabric. For example, the higher to lower backscatter transitions in the northern half of the survey match transitions between 'mega-ripples' and 'fine rippled' categories (Fig. 8C). Note also the correspondence of the 'bed rock & boulder' categories with the striated sidescan of the central high area, and also on the lesser northern high. These two areas were also marked by the occurrence of abundant Zoanthidea (Fig. 8D).

The *Autosub6000* mission to the Haig Fras area provided a successful demonstration of AUV seafloor habitat mapping in an open shelf setting, with near-bottom current speeds and turbidity being appreciably higher than encountered in comparable deep-water operations. The photographs obtained were effective in both assessing the seabed

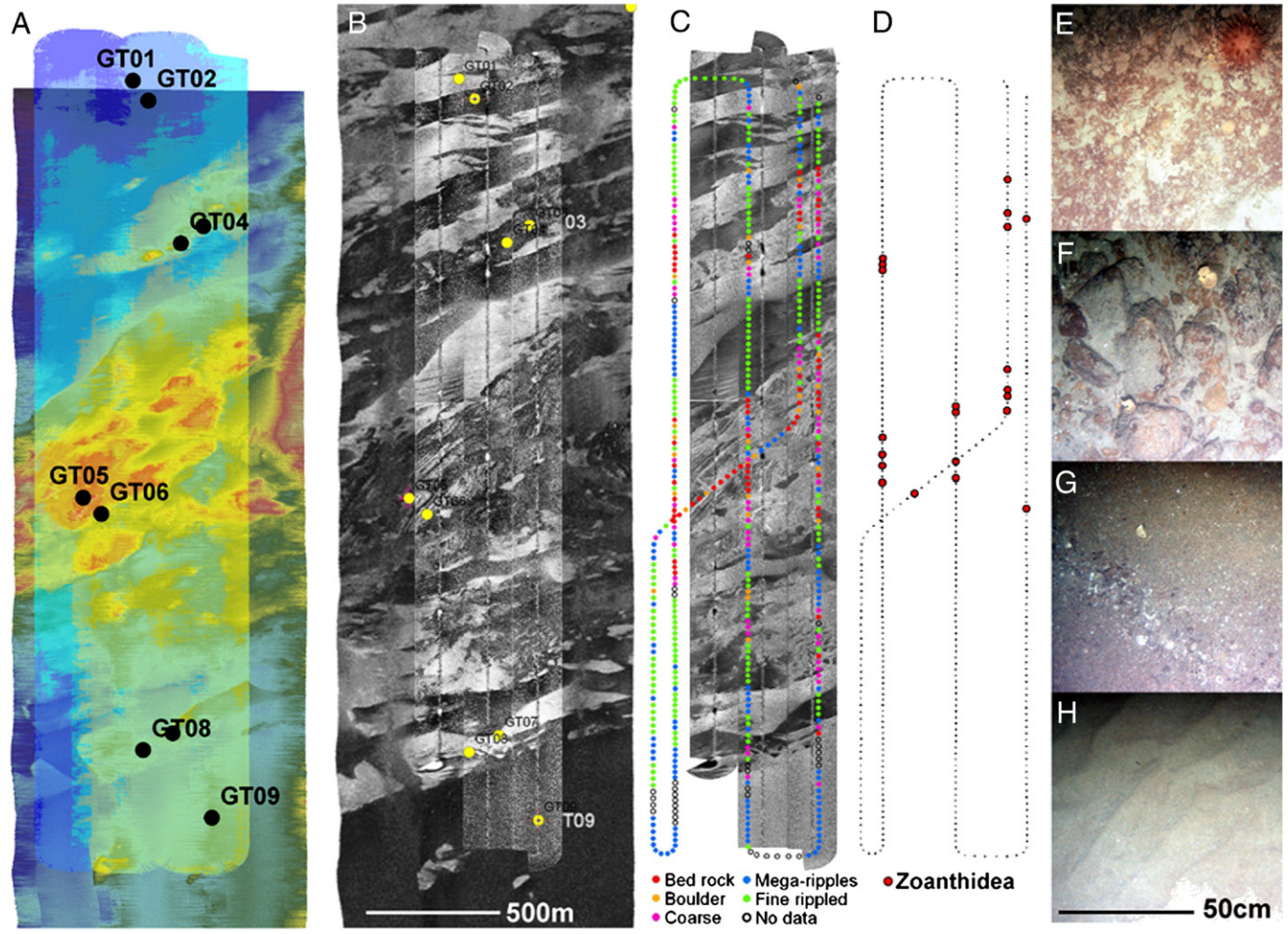

Fig. 8. *Autosub6000* survey in the Haig Fras area. (A) AUV MBES overlain on *RV Cefas Endeavour* MBES data (reds, topographic highs; blues, lows). (B) AUV high-frequency SSS over vessel MBES backscatter data (dark, high backscatter; light, low). (C) Photographic seabed classification over AUV SSS (note reversed phase; dark low backscatter, light high). (D) Occurrence of abundant colonial anemones (Zoanthidea). (E–F) Example seabed classification images: bedrock, boulder, mega-ripples, fine rippled. (Scale: A–D, as inset on B; E–H, as inset on H).

fauna and classifying seabed types for habitat mapping purposes. The close match between the photographic seabed classification and variations in seabed acoustic fabric (high frequency SSS) suggests that the joint use of camera and SSS systems on an AUV platform may be particularly effective in providing well ground-truthed habitat maps. A repeat AUV survey to Haig Fras is scheduled for autumn 2014 to assess geomorphological and biological change over a two-year timescale; further repeats will be undertaken in future years once the site is fully designated as a Marine Protected Area and management measures are implemented.

AUVs have already been used to assess effectiveness of management measures in deep-water environments. In May/June 2011, the NERC *Autosub6000* AUV was used to investigate several known ecosystem hotspots off northwest UK, in order to guide the design of appropriate conservation measures and management plans (Huvenne et al., 2011a). Here, we show a dataset from the Darwin Mounds — small cold-water coral mounds (up to 5 m high, 75 m across) located at 1000 m WD in the northern Rockall Trough. The mounds were discovered in 1998 during a broad-scale environmental mapping survey for the Atlantic Frontiers Environmental Network (AFEN) programme (Bett, 2001; Masson et al., 2003). Follow-up surveys in 1999 and 2000 revealed that many of the mounds were damaged by bottom trawling (Wheeler et al., 2005). As a result of these observations, the area was closed in 2003 to all bottom contact fisheries through an emergency procedure under the EU Common Fisheries Policy — a situation made permanent in 2004 (De Santo and Jones, 2007). The area is currently designated as a Site of Community Interest, and will become the first UK deep-water Special Area of Conservation (SAC) under the EU Habitats Directive.

No further scientific surveys took place in the Darwin Mounds area until the *Autosub6000* data acquisition in 2011, which allowed their status to be re-evaluated after eight years of protection. Two sections of the Darwin Mounds were mapped using *Autosub6000* in multiple passes, to create a multi-frequency acoustic dataset for advanced automated habitat classification (Huvenne et al., 2011a). The first pass of the AUV used the EM2000 MBES at 100 m altitude to create a bathymetric and backscatter map with 2 × 2 m and 0.5 × 0.5 m pixel resolution, respectively (Fig. 9A,B). In the second pass, the 120 kHz SSS was used, again at 100 m altitude, resulting in a map with 0.5 × 0.5 m pixels (Fig. 9C). Finally, during the third pass, which took place during a separate dive, 410 kHz SSS data were collected at an altitude of 15 m (Fig. 9D). Mapping times for the same 7 × 1.5 km box were 10 h for MBES, 5 h for low-resolution SSS and 16 h for high-resolution SSS. The highest resolution SSS data can be processed to a pixel size of 0.05 × 0.05 m, based on the across-track capabilities of the system under the given survey configuration (Fig. 9F).

It is clear that for mapping of specific features such as cold-water coral colonies (and potentially identifying live coral stands from their backscatter response), ultra-high-resolution mapping data are essential (Fig. 9F), even if they are more time-consuming to collect. The new *Autosub6000* AUV data can also be compared with the original deep-towed SSS data (Fig. 9E), which were of similar resolution and

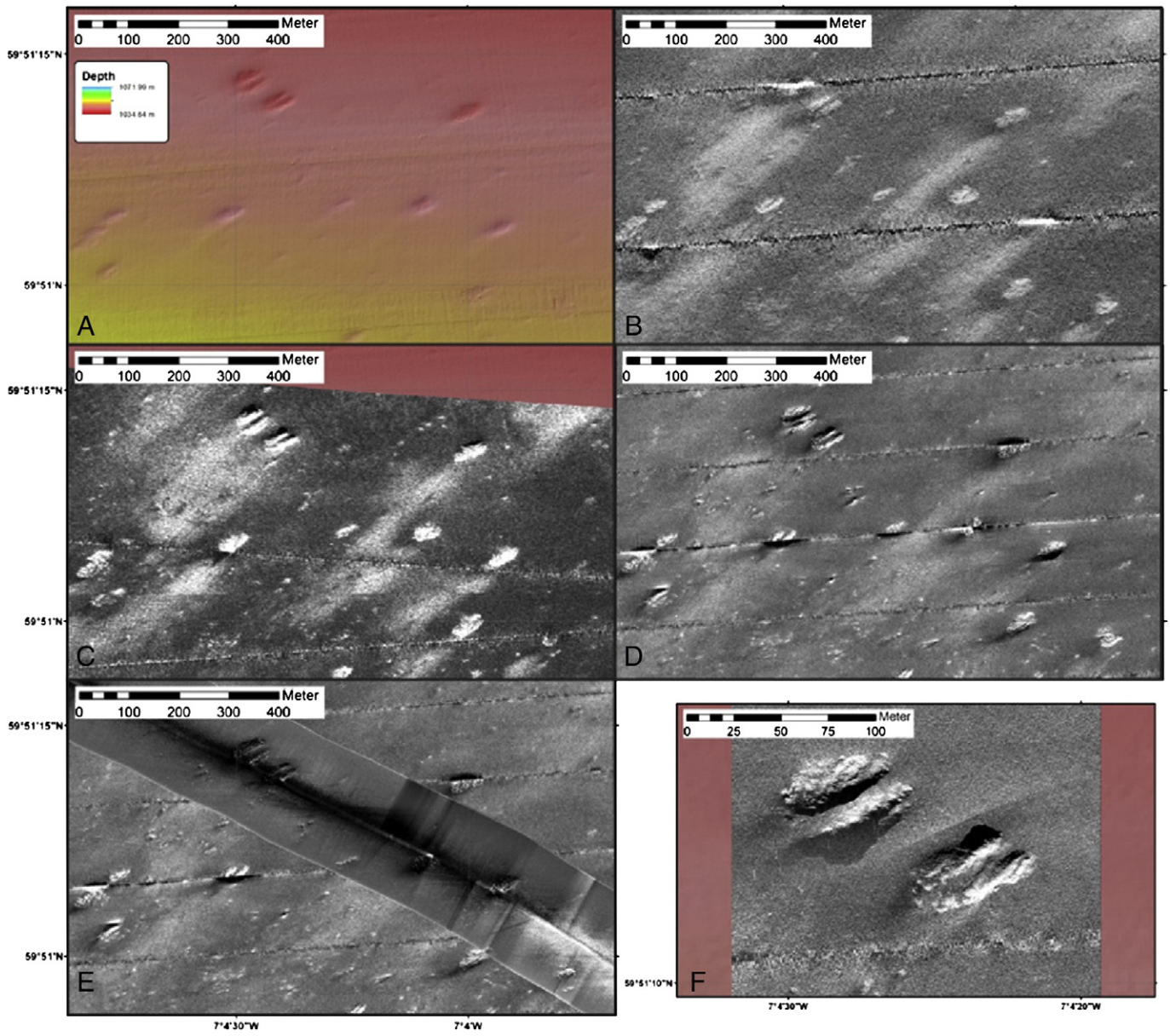

Fig. 9. *Autosub6000*-based maps of the Eastern Darwin Mounds in the northern Rockall Trough, northeast Atlantic. (A) EM2000 bathymetry, 2 × 2 m pixels, showing the morphology of individual mounds; (B) EM2000 backscatter, 0.5 × 0.5 m pixels, showing high backscatter mounds and sediment tails; (C) EdgeTech 2200 FS 120 kHz SSS map, 0.5 × 0.5 m pixels; (D) EdgeTech 2002 FS 410 kHz SSS map, 0.2 × 0.2 m pixels; (E) strip of historical GeoAcoustics 410 kHz SSS data overlaying the previous map, allowing comparison of trawl marks before and after fisheries closure, 0.5 × 0.5 m pixels (after Wheeler et al., 2005); (F) EdgeTech 2200 FS 410 kHz SSS data processed to its finest resolution, 0.05 × 0.05 m pixels. All SSS and MBES backscatter data are processed with the NOC in-house software PRISM (Le Bas and Hühnerbach, 1999). Light tones represent high backscatter; dark tones indicate low backscatter.

frequency (GeoAcoustics 100 and 410 kHz data, 0.5 × 0.5 m pixel, Wheeler et al., 2005); this allows the persistence of trawl marks and potential changes in the spatial distribution of live and dead coral to be assessed (Huvenne et al., 2011a). Elsewhere, cold-water coral colonies on the continental slope at 600–900 m WD have been mapped with the *C-Surveyor-II*™ AUV on Great Bahama Bank (Grasmueck et al., 2006) and at the base of the Miami Terrace, off southeast Florida (Correa et al., 2012).

Finally, integration of high-resolution colour camera systems on to AUVs is providing unprecedented insights into the spatial distribution of deep-sea fauna. In July 2012, the NERC *Autosub6000* AUV was used to investigate spatial distribution patterns of sessile and mobile megafauna in relation to topographic and other spatial features at ~4.8 km WD on the Porcupine Abyssal Plain, northeast Atlantic. A high-resolution colour photographic dataset was collected in order to evaluate how community structure, biodiversity and ecosystem functioning scale with observable habitat features (both from photographs and shipborne MBES data). The aim was to address some of the major unresolved questions about the importance of analytical scale in determining biological community relationships (e.g. Nakazawa et al., 2011).

The AUV photo survey covered a range of spatial scales (Fig. 10A), including a broad-scale grid (10 × 10 km) and three fine-scale grids (1 × 1 km area with 100 m track line spacing). The broad-scale grid was positioned to allow coverage of an abyssal hill and surrounding flat seafloor, which were imaged on previously collected shipborne MBES data; two of the fine-scale grids were nested within this area, and a third was located to the south (at the Porcupine Abyssal Sustained Observatory site; Lampitt et al., 2010). Over 165 km of continuous image transects were taken with the AUV, although technical issues resulted in no images being obtained across the abyssal hill. In total over 175,000 downwards-facing images were obtained during ~50 h of AUV seabed operations (with >160,000 of these images being within

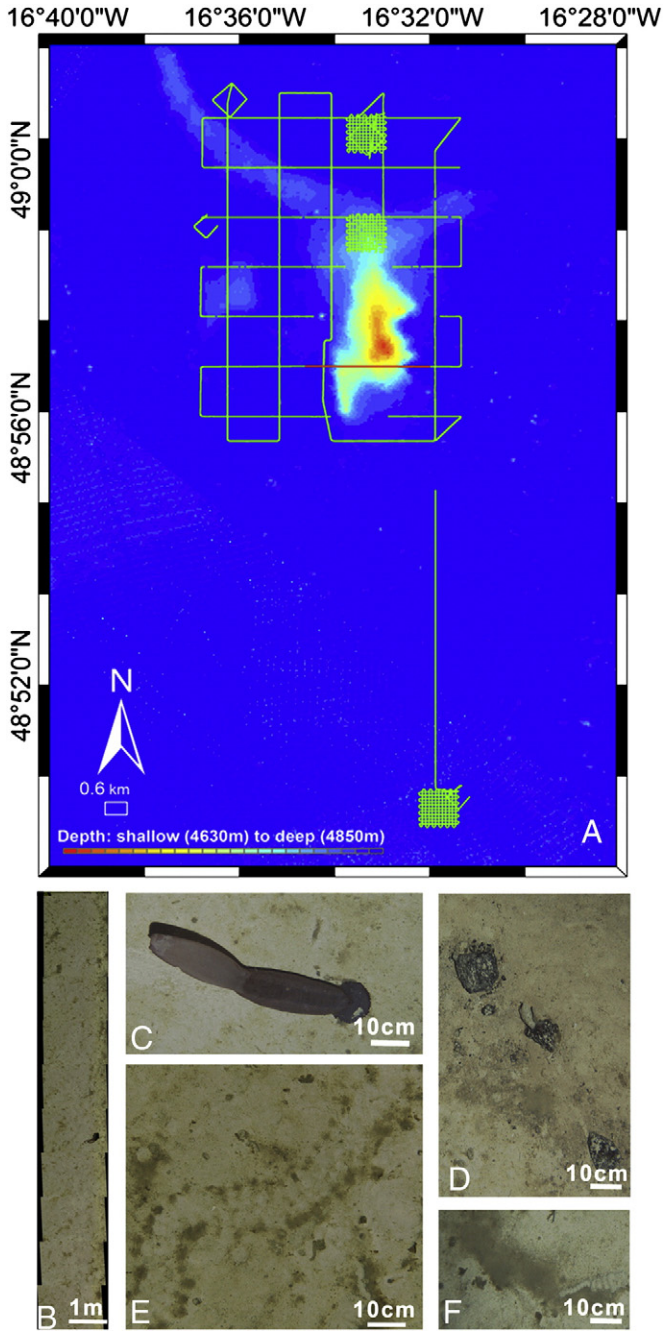

Fig. 10. *Autosub6000* survey data from the Porcupine Abyssal Plain, northeast Atlantic. (A) Bathymetry map — green lines depict *Autosub6000* photographic missions, red lines depict the towed camera WASP line; (B) example tile image with a *macourid* fish and visible organic detritus patches; (C) observed *Psychropotes longicauda*; (D) example of geological features, i.e. small rocks on the seafloor; (E) example of bioturbation patterns, expected to have been created by *Psychropotes longicauda*; (F) phytodetritus patches, illustrated by darker patches of seabed and holothurian faeces.

the correct range for subsequent analysis). Post-processing, including optical backscatter, non-uniform illumination, colour, positional corrections and geo-referencing, was performed on individual images. Ten images were then mosaicked together to create a single image tile in which overlap is eliminated (Fig. 10B), resulting in over 15,000 tiles in Geo-TIFF format.

Examination and annotation of the tiles have enabled the following analyses to be undertaken: i) mapping and measurement of individual benthic organisms (Fig. 10C) and geological features (Fig. 10D) at mm-scale resolution, ii) fine-scale analysis of particulate organic carbon cover (i.e. food resource) across the survey area (Fig. 10F), using an automated percentage-cover analysis, iii) mapping of fine-scale seafloor sedimentary processes, including bioturbation as indicated by animal traces (Fig. 10E), and iv) analysis of AUV image data in conjunction with habitat maps (generated from shipborne MBES bathymetry and backscatter, and sediment cores). Deployment of the AUV has therefore enabled an abundance of high-resolution photographic data to be collected over an extensive area of deep ocean floor in a relatively short time period; this has provided new insights into seafloor character and habitat relationships from cm^2 to km^2 scales, something which has not previously been achieved in the deep ocean.

3.4. Seafloor morphology associated with bedforms, scours and scarps

AUVs have been used to map a variety of seafloor morphological features, including beneath ice sheets beyond the reach of research vessels. For example, Jenkins et al. (2010) used the NERC *Autosub3* AUV to investigate the retreat of Pine Island Glacier (PIG) in West Antarctica. The AUV undertook six missions, totaling 510 km of track-line collected over 94 h, beneath the PIG ice shelf at distances of up to 50 km from the ice front. AUV MBES mapping revealed a transverse ridge at 700 m WD between the present-day ice front and grounding line, interpreted to be a former grounding line. Additional sensors on the AUV included temperature, salinity, dissolved oxygen concentration and light attenuation, which provided information on seawater properties beneath the ice. The study provided important new insights into the processes driving rapid loss of ice from this sensitive region (and the potential impacts on global sea level), as well as the most extensive seafloor mapping dataset collected with an AUV from beneath an ice shelf. Graham et al. (2013) subsequently used the same dataset to map seafloor 'corrugations' and iceberg ploughmarks over the transverse ridge discovered in the above study. The data contributed to a test of contrasting hypotheses for genesis of the corrugations, which has implications for the reconstruction of the ice shelf in the Holocene. Dowdeswell et al. (2008, 2010) used the NERC *Autosub2* AUV to map glacial bedforms at 840 m WD on the floor of Kangerlussuaq Fjord, which were generated by the fast-flowing Kangerlussuaq Glacier. These data supported the finding that the Greenland Ice Sheet extended throughout this fjord system during the Last Glacial Maximum. This mission was also notable for the first integration of a digital camera system onto the AUV (which was flown at altitudes of <10 m), revealing the presence of ice-rafted dropstones and a variety of benthic fauna on the seabed at cm-scale resolution.

AUV mapping can also be used in studies of seafloor deformation. Larroque et al. (2011) used an AUV to collect high-resolution MBES data (2 m gridding) in order to characterise the active tectonic and gravitational deformation on the northern Ligurian margin, western Mediterranean. In particular, the AUV MBES data were able to image a 10 m-high fault scarp on the seafloor that was not seen on shipborne MBES data; these new data contributed to increased knowledge of relationships between active deformation and seismicity, and regional seismic hazards. Eddy Lee and George (2004) used a *Hugin 3000* AUV equipped with MBES, SSS and SBP to map the Sigsbee Escarpment in the Gulf of Mexico at 1300–2200 m WD. A series of interesting seafloor features was imaged, including fault scarps, slump deposits, and erosional furrows; these were associated with salt tectonics, gravity-driven mass failure, and bottom current activity, respectively. Further examples of AUV data being applied to studies of seafloor deformation can be found in Caress et al. (2008).

A number of studies have taken advantage of the higher resolutions achievable when AUV mapping to investigate gravity-driven flow processes on continental margins. For example, the NERC *Autosub6000* AUV was used to survey four zones of giant erosional scours associated with submarine canyons and channels along the northeast Atlantic continental margin from Morocco to Biscay; this was the first study to use an AUV for high-resolution imaging of truly deep-water scours

(>4000 m WD), and was the first scientific deployment of the *Autosub6000* vehicle (Huvenne et al., 2009; Macdonald et al., 2011). The scour fields were imaged with a Kongsberg Simrad 200 kHz EM2000 MBES mounted on the AUV. The AUV undertook missions of about 24 h duration and was flown 100 m above the seabed, collecting bathymetric data over an area of ~25 km^2 with a horizontal resolution (pixel size) of 2 m and vertical resolution of 0.15 m. Upon recovery of the vehicle, data were uploaded and processed, and bathymetric maps suitable for planning of subsequent coring locations were generated within 2 h. The high-resolution AUV imagery provided new insights into scour genesis, revealing how relatively small, isolated, spoon- or v-shaped scours a few hundred metres across underwent lateral expansion to form larger areas of amalgamated scour covering several kilometres (Fig. 11).

Normark et al. (2009) used the *D. Allan B.* to collect high-resolution mapping data across giant scours on the Redondo Fan in the San Pedro Basin offshore California. MBES data achieved 1.5 m horizontal resolution and 0.3 m vertical accuracy, while SBP data achieved 0.1 m vertical resolution; ground-truthing data were provided by ROV vibracores. The aim was to image linear sets of giant scours within a channel system at 600–700 m WD (previously imaged with shipborne MBES data), in order to understand flow processes operating within the channels. The AUV produced spectacular MBES maps of the scours, which are up to 200 m wide and 30 m deep and appear to be a good example of erosional cyclic steps. These AUV data allowed the history of channel development to be reappraised, and emphasised the importance of erosional processes in this system.

Similar high-resolution AUV mapping of the Lucia Chica channel system, off the Pacific coast of California, was undertaken with the MBARI *D. Allan B.* AUV (Maier et al., 2011, 2012). The AUV data (1 m horizontal resolution and 0.3 m vertical resolution) led to a fundamental reappraisal of the nature of this channel system, which had previously been imaged with a shipborne MBES with ~50 m horizontal resolution (Greene et al., 2002; Paull et al., 2002). AUV MBES and SBP data covered an area of ~70 km^2 from 930 to 1250 m WD, revealing a complex series of discontinuous distributary channels with varying morphologies being fed by a single sinuous channel. The new high-resolution data revealed that submarine channel systems show complexity below the spatial resolution of shipborne imaging systems, and subsequently contributed to a general model for channel inception and evolution in the deep sea (Fildani et al., 2013).

AUVs have also been used to image sedimentary features within submarine canyons. Paull et al. (2013) again used the *D. Allan B.* to collect high-resolution MBES (0.7 m lateral resolution) and SBP (0.1 m vertical resolution) data from La Jolla Canyon, offshore southern California, in order to understand the processes responsible for generating observed morphologies at a scale comparable to outcrop. Subsequent ROV dives were used to ground-truth AUV data and to provide vibracore samples for sediment dating. The AUV data revealed fine-scale relief that was not visible on existing shipborne MBES data at >10 m grid resolution. Visible features include crescent-shaped bedforms on the canyon floor, which are 1–2 m high and typically found on slopes of ~1.0° (Fig. 12); vibracoring of the seabed in the vicinity of these bedforms destabilised surrounding sediments, apparently as a result of

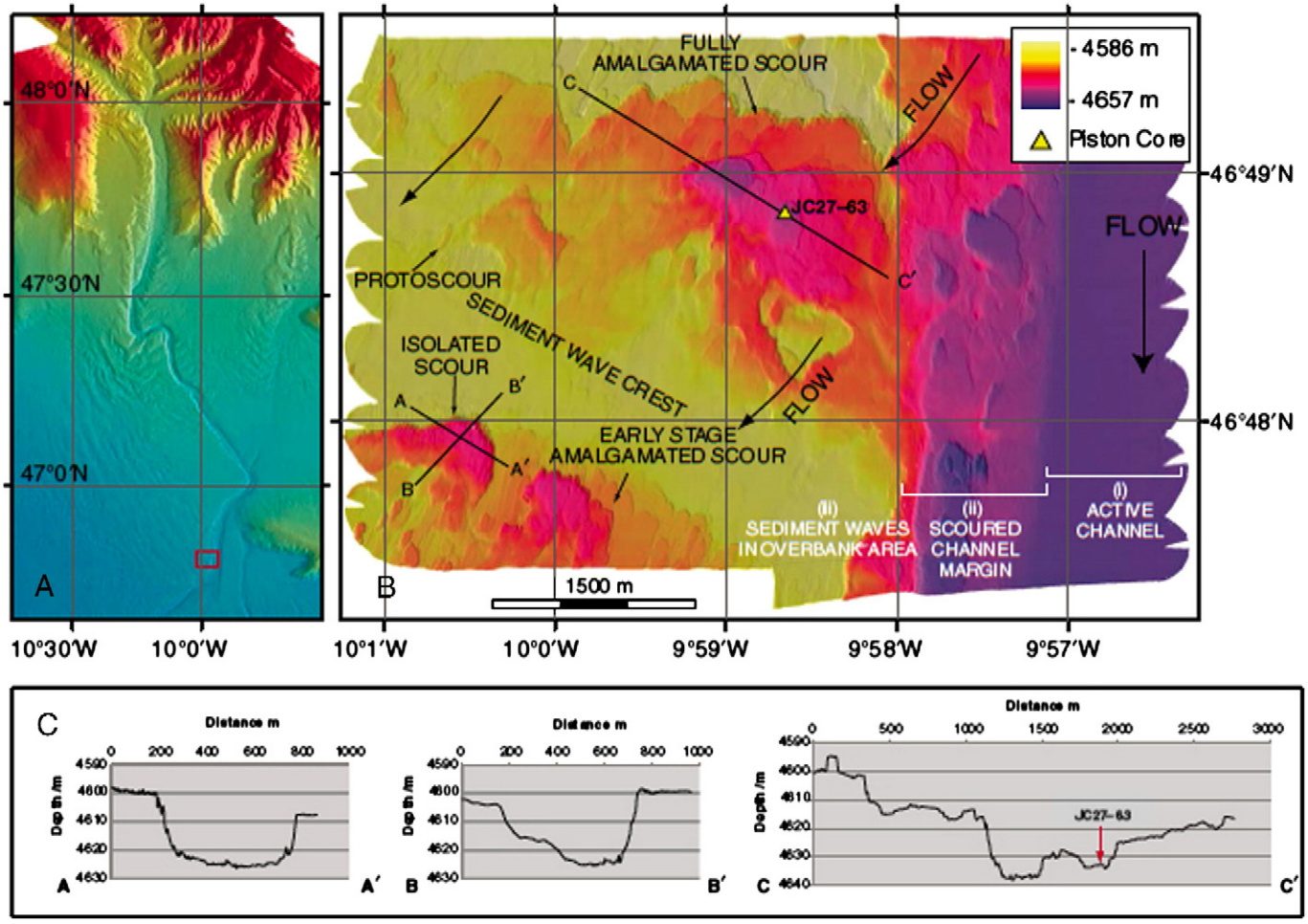

Fig. 11. Giant scours and overbank sediment waves adjacent to Whittard Channel. Location map (A) shows 3D shipborne MBES data over Whittard Canyon–Channel in the northern Bay of Biscay. Red box shows AUV survey area. High-resolution AUV MBES data (B) show details of the sours and intervening sediment wave crests, adjacent to the main channel. Cross-sectional profiles (C) show 2D morphology of the scours.

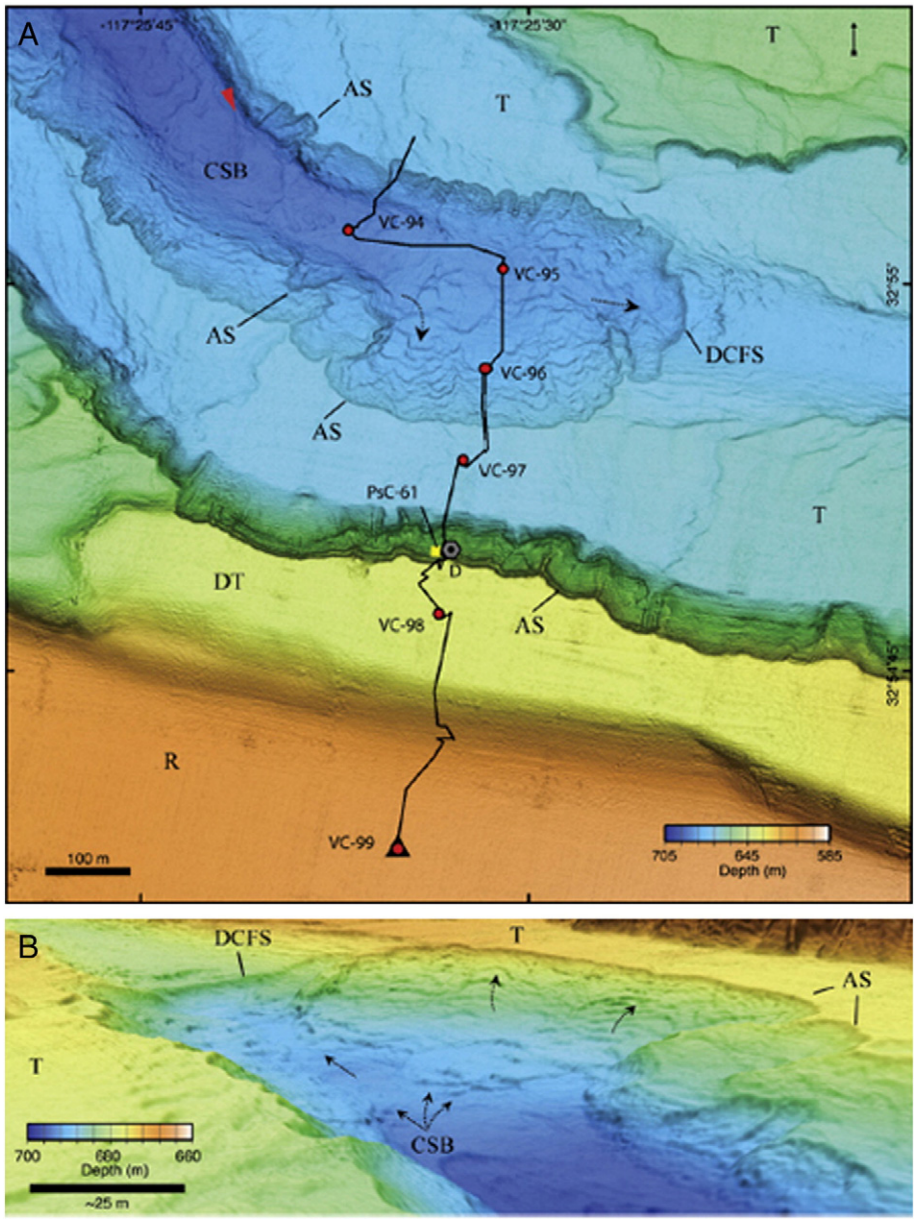

Fig. 12. (A) Map showing AUV MBES data from a section of La Jolla Canyon. Path of ROV dive is shown by black line, with vibracore locations (VC) marked by red circles and a push core transect (Psc) marked by a yellow square. Note the smooth terraces outside (R) and adjacent to the canyon thalweg (DT, T), abundant arcuate scarps (AS) on the canyon margin, a distinctive canyon floor arcuate scarp (DCFS), and trains of crescent-shaped bedforms (CSB) on the canyon floor. Black arrows show locations of CSB with varying orientations. Red arrow shows orientation of perspective image shown in (B), with a VE ×2.
From Paull et al. (2013).

liquefaction (see video in Supplementary information in Paull et al., 2013). Sediment dating provided evidence for recent canyon activity, which could suggest the bedforms are generated by turbidity currents. However, the detailed AUV MBES data support a recent hypothesis, developed and explored during AUV mapping studies of Monterey Canyon (Paull et al., 2010, 2011), that these features are generated by episodic movement (breaching) of the unconsolidated sediment fill of the canyon floor.

A major hindrance in the interpretation of sedimentary features in submarine canyons and channels is the lack of direct observations of their formative processes (Talling et al., 2013). Submarine density flows that carve canyons and channels, and commonly generate scours and bedforms, are amongst the most poorly understood flows on Earth, with velocity data restricted to just a handful of locations (Talling et al., 2012, 2013). Furthermore, such velocity data are almost entirely restricted to single-point vertical profiles of downstream velocity (Khripounoff et al., 2003; Vangriesheim et al., 2009; Xu et al., 2013); this is in sharp contrast to the spatially continuous Acoustic Doppler Current Profiler (ADCP) derived cross-sectional data typically obtained for other channel types, such as rivers and tidal channels (Dinehart and Burau, 2005; Parsons et al., 2007; Vennell and Old, 2007). In part, this data scarcity is a function of the infrequent and highly destructive nature of submarine density currents. However, there are also prominent methodological issues in collecting two- and three-dimensional cross-sectional velocity data in these submarine flows. The ADCP is the instrument of choice for spatially continuous velocity sections, yet dependent on the specific beam orientations of a given ADCP design, side lobe interference from the sea-floor means that the lowermost 8 to 15% of the measurement depth is of insufficient quality (Simpson, 1986; Gordon, 1996). Therefore measurements cannot be collected in this basal zone, which is the primary zone of interest for understanding density currents. This limitation has restricted ship-mounted ADCP

measurements of density currents to shallow lakes of the order of a few tens of metres deep (Best et al., 2005; Wei et al., 2013). In deeper water, ADCPs can be towed in order to lower the instrument closer to the sediment surface enabling density current measurements (Parsons et al., 2010). However towing is limited to relatively shallow water, and there are issues regarding the stability of the acoustic tow-fish, the difficulty in accurately repeating survey lines, operation in adverse weather, and difficulties in towing close to the bed over complex topography. AUV mounted ADCPs have enormous potential to address these issues and record density flows across the oceans at a wide range of flow depths. Here we provide a new example of such a deployment to measure an active submarine channel density current.

A prominent active submarine channel network is present on the Black Sea shelf immediately north of the Bosphorus Strait, at 70–120 m WD, fed by denser, higher-salinity, northward flowing Mediterranean-derived water exiting the strait (Flood et al., 2009). In May 2010, the *RV Koca Piri Reis* was used to launch the *Autosub3* AUV to study this channel system. *Autosub 3* carried a 1200 kHz ADCP, operating with a vertical bin size of 0.5 m. The ADCP data shown here were collected along a 3.5 km-long cross-channel transect close to where the flow exits the mouth of the Bosphorus Strait (Fig. 13), during a 48-hour mission starting on 22 May 2010. The position of this line illustrates another key advantage of AUV technology, since it is right in the mouth of the narrowest international shipping lane on Earth, and therefore a position where a towed ADCP could not be realistically deployed.

ADCP velocity data from an AUV require considerable processing in order to account for i) any drift in the inertial navigation system, ii) changes in depth of the AUV relative to the seabed, and iii) side lobe interference near the seafloor; data also need to be adjusted into a global coordinate system. In the present case, data were subsequently rotated so that downstream and cross-stream velocities are parallel and perpendicular to the channel walls respectively. Fig. 13 shows the

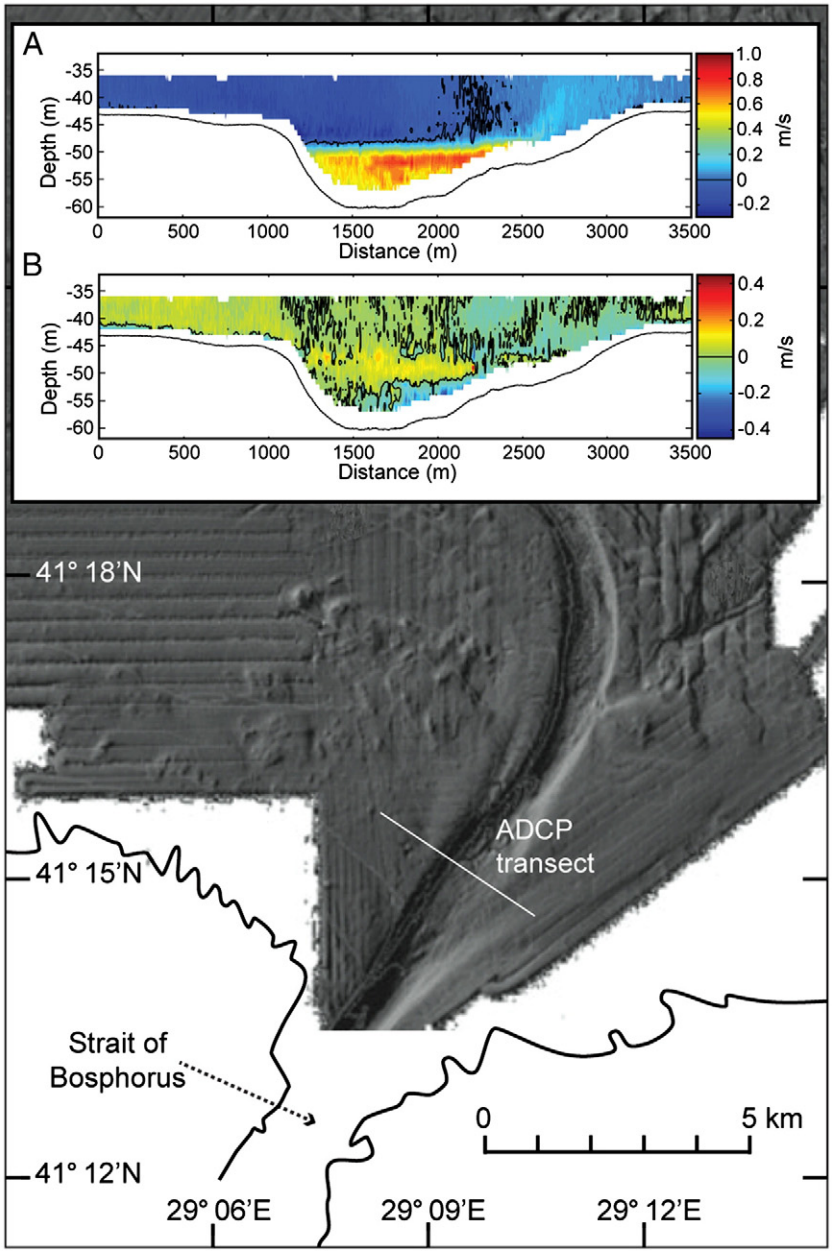

Fig. 13. Bathymetric map of the seafloor at the northern mouth of the Bosphorus, showing a large seafloor channel (modified from Flood et al., 2009). The survey line, shown in white, shows the position of the AUV mounted ADCP transect. Insets show (A) the downstream, and (B) the cross-stream velocity flow fields. For the cross-stream (B), positive numbers show outer bank directed flow, and negative numbers inner bank orientated flow.

downstream and secondary velocity fields at the entrance to a large submarine channel bend. The downstream flow field shows a flow about 15 m thick with maximum velocity (0.9 ms^{-1}) close to the upper surface of the flow. The secondary circulation shows a single circulation cell with basal flow towards the inner bank, and overlying flow towards the outer bank (Fig. 13B). Such data provide huge advantages over single-point vertical velocity profiles, since bend flow has been shown to be highly three-dimensional making interpretation of single-point profiles problematic (Giorgio Serchi et al., 2011). Examination of high quality velocity data at different points around a bend can also be used to assess the nature of the helical flow field in submarine channels (Wei et al., 2013), and in particular to examine whether this flow field pattern is reversed relative to that in river channels (Corney et al., 2006, 2008; Parsons et al., 2010; Dorrell et al., 2013).

In conclusion, AUVs are an optimal solution for collecting spatial velocity data in water depths ≥100 m; these data are essential for correct evaluation of the mechanics of sediment transport, surface grain sorting, and deposit formation in active systems. AUVs provide a stable platform for measurement, and recent technological advances within this field are opening up an array of possibilities for the study of a wide range of flow types in the deep ocean.

4. Future applications

4.1. New drivers

There are a number of new scientific, industrial, political and economic drivers that will ensure that demand for AUVs in marine geoscience is likely to increase further in the future. In the scientific domain there is now a constant push for higher resolution mapping and imaging data, particularly in deep water where access to such data is providing new insights into a variety of geological processes (particularly volcanic and sedimentological). Industry drivers include the push into deeper water by the hydrocarbons sector (e.g. Eddy Lee and George, 2004), the recent development of offshore renewables and carbon capture and storage (CCS) facilities in shelf waters (e.g. Bickle et al., 2007), the future exploitation of deep-sea mineral resources, and the positioning of seafloor fibre-optic cables for telecommunications and seafloor observatories (Caress et al., 2008). All of these sectors require high-resolution mapping data for geohazard analysis (e.g. landslides, fluid escape features, mobile substrates), environmental impact assessments, and environmental monitoring (e.g. leaking hydrocarbons/CO_2 and repeat monitoring of benthic habitats and ecosystems). For example, the WHOI *SENTRY* AUV was recently used to map the hydrocarbon plume resulting from the Deepwater Horizon oil spill in the Gulf of Mexico (Camilli et al., 2010), and assess the impact on benthic fauna and habitats. Military drivers include mine counter measures and rapid environmental assessment, particularly in hostile regions where covert operations are required (e.g. Bovio et al., 2006; Hagen et al., 2008). Political drivers include the requirement to establish new Marine Protected Areas (e.g. De Santo and Jones, 2007) and co-ordinated marine monitoring programmes (e.g. the EU Marine Strategy Framework Directive). These will require national governments to divert extra resources into marine mapping and monitoring. However, economic drivers, particularly rising vessel fuel oil costs, are ensuring that AUVs are increasingly being seen as a cost effective way to generate data of sufficient quality to meet statutory obligations (e.g. Wynn et al., 2012).

To give an example of multiple drivers, the Sleipner CCS project in the North Sea involves the injection of CO_2 into a saline aquifer within the Utsira Sand Formation. The operation is run by Statoil, and is currently the only commercial level system in operation in the European marine sector. To date the reservoir has received more than 12 million tonnes of CO_2, and models and seismic observations show that the CO_2 moves through the formation, which has a total area of more than 1400 km^2 (Bickle et al., 2007). The use of submarine reservoirs (aquifers or old and gas fields) is subject to strict environmental monitoring to ensure a minimal impact on the marine system. Such monitoring of spatially extensive CCS reservoirs has to be cost effective; traditional ship surveys would be prohibitively expensive for this purpose. It has been proposed that a suite of sensors for detecting leakage could be deployed on a number of AUVs that would then be used for frequent, high temporal scale studies over the areas of possible leakage. This is the only possible cost effective way of meeting what will be strict environmental monitoring requirements for the commercial scale development of marine CCS projects. For further details see the EU ECO_2 project (www.eco2-project.eu).

4.2. New vehicles

As the range of new drivers for AUV use has increased, so has the diversity of vehicle types. Several vehicles have been developed that have a hovering capability, principally for use in shallow water and largely targeted at military use or maintenance of hydrocarbon production infrastructure. However, Kantor et al. (2008) describe a new hovering AUV *DEPTHX* that was developed using NASA funding, in order to explore and characterise the unique biology of the world's deepest known limestone sinkhole in Mexico. A hovering capability could prove highly beneficial in topographically complex submarine environments such as submarine canyons, where fully 3D mapping has previously only been possible with an ROV (e.g. Huvenne et al., 2011b). Until recently, existing AUVs have had a maximum depth rating of 6000 m. However, WHOI have developed *Nereus*, a hybrid AUV/ROV for scientific exploration down to the very deepest parts of the ocean, up to 11,000 m WD; this is almost twice the depth range of any existing AUV (Bowen et al., 2008). The vehicle can swim freely as an AUV for seafloor mapping purposes, but can also be tethered to the ship for real-time video surveys and seafloor sampling/experiments.

To meet the need for increased endurance, NOC has developed a new long range AUV *Autosub Long Range*, that is intended to bridge the capability gap between AUVs and gliders (Furlong et al., 2012). It is a relatively slow-moving propeller-driven vehicle with a depth rating of 6000 m and an endurance of ~6000 km or six months. The vehicle is initially being equipped with low-power sensors such as CTD and a 300 kHz ADCP, mostly for oceanographic studies. However, future developments of the NERC-owned vehicle include a seabed hibernation capability, ideal for long-term monitoring of seafloor environments during a single multi-month deployment and/or reactive monitoring of rare events, e.g. benthic storms. A further development is the concept of air-launched AUVs that can be deployed from an aircraft. Although most studies have focused on aerial deployment of traditional *REMUS*-type vehicles, e.g. Pan and Guo (2012), a recent NERC-funded project investigated the use of highly portable small-scale AUVs, weighing just 2.5 kg but with a range of 350 km at speeds of 0.5 ms^{-1} (Stevenson, 2011). Such vehicles could one day be used to respond rapidly to extreme events, e.g. an oil spill, a harmful algal bloom, or a submarine volcanic eruption.

4.3. New sensors

Most seafloor mapping requirements have been met through development of MBES, SSS and SBP systems that can be deployed on an AUV, supported by seafloor photography. New sensor developments are therefore likely to be focused on water column monitoring. The first deployment of a geochemical sensor on an AUV was in 2000, when the NERC *Autosub* AUV was fitted with an in situ dissolved manganese analyser (Statham et al., 2003, 2005). This deployment demonstrated how AUVs carrying chemical sensors can detect small-scale variability of distributions of chemical species that would not be resolved by conventional sampling approaches. Since then, chemical sensors on AUVs deployed for marine geoscience purposes have principally been used when searching for active hydrothermal plumes in the water column (e.g. Yoerger et al., 2007a; German et al., 2008b; Connelly et al., 2010)

or for detecting active methane venting from pockmarks (Newman et al., 2008). However, new drivers such as CCS are leading to new sensors being developed, e.g. to monitor CO_2 leakage from subsurface CCS reservoirs.

4.4. New approaches to risk, reliability, and AUV management

There is a growing requirement for increased reliability of AUVs in the scientific sector, due to the high value of the bespoke vehicles being deployed and the data being obtained. This has generated a number of studies designed to evaluate and manage risk associated with AUV deployments (e.g. Brito et al., 2012). As AUV use increases in the future, there will also be greater demand for clarity around legal issues and diplomatic clearance; these requirements will differ for different users, i.e. marine scientific research, military data gathering and commercial surveys. There are still many uncertainties as to the legal definition of an AUV, i.e. whether or not is classed as a 'ship'. This definition will be important when dealing with issues such as collision risk, salvage, and navigation failure leading to unauthorised entry into foreign waters.

5. Conclusions

In the last 15 years, AUVs have rapidly emerged as a vital tool for marine geoscientists, especially those involved in seafloor mapping and monitoring. The ability of these vehicles to fly at relatively low altitude over the seabed enables them to collect spatial data at far higher resolution than surface vessels, especially in deep water. When used in conjunction with other platforms as part of a nested survey, a complete package of regional vessel-based mapping, high-resolution targeted AUV survey, and ROV video ground-truthing and sampling can be deployed. In addition to seafloor mapping, AUVs have been used to detect expelled hydrothermal or cold seep fluids in the water column. Continued development of new vehicles and sensors will increase the range of marine geoscience applications, while advances in artificial intelligence will increase reliability and flexibility. AUVs are already capable of making decisions that allow them to avoid seafloor or under-ice collisions, and increasingly these vehicles are developed with sufficient intelligence that they can adapt their surveys according to changes in the environment they are monitoring, e.g. discovering a hydrothermal plume (Bellingham and Rajan, 2007; Yoerger et al., 2007a). When combined with new drivers such as Marine Protected Area monitoring and site surveys for offshore renewable installations, it is clear that AUVs will continue to play an increasingly important role in the exploration and monitoring of the oceans.

Acknowledgements

We are grateful to the Editor, David Piper, and two anonymous reviewers for useful suggestions that helped to improve the manuscript. JEH benefited from funding from the NERC Marine Renewables Knowledge Exchange (MREKE) programme. The new NERC *Autosub6000* AUV data described in the paper were collected by staff based at the Marine Autonomous and Robotic Systems (MARS) facility at the National Oceanography Centre, Southampton. We thank these staff for their hard work and professionalism during data collection, especially Gwyn Griffiths, Steve McPhail, Maaten Furlong, Miles Pebody, Pete Stevenson, James Perrett and Dave Paxton. We also thank all staff associated with operation of the NERC research vessels RRS *James Cook* and RRS *Discovery*, which were the ships most commonly used for *Autosub6000* deployment and recovery.

Autosub6000 data collection from Cayman Trough was funded by NERC grants NE/101442X/1 and NE/F017758/1. Data collection from Haig Fras was funded by Defra project MB0118 and the NERC MAREMAP programme. We are also grateful to Cefas for providing the shipborne bathymetric data from the Haig Fras site that contributed to this case study. Data collection from the Darwin Mounds was funded by the NERC MAREMAP programme, EU FP7 HERMIONE (grant no. 226354) and ERC CODEMAP (grant no. 258482), while ROV hire was funded by JNCC and the Lenfest Ocean Programme (PEW Foundation). Data collection from the Porcupine Abyssal Plain was funded by NERC grant NE/H021787/1. *Autosub6000* ADCP data collection in the Black Sea was funded by NERC grants NE/F020511/1, NE/F020120/1 and NE/F020279/1. We also thank Rick Hiscott and Ali Aksu of Memorial University, Canada, Roger Flood of Stony Brook University, USA, and Dogan Yasar of Dokuz Eylül University, Turkey, along with the Master and crew of the *RV Koca Piri Reis* for their assistance with cruise planning and operation.

References

Armstrong, R.A., Singh, H., Torres, J., Nemeth, R.S., Can, A., Roman, C., Eustice, R., Riggs, L., Garcia-Moliner, G., 2006. Characterizing the deep insular shelf coral reef habitat of the Hind Bank marine conservation district (US Virgin Islands) using the Seabed autonomous underwater vehicle. Continental Shelf Research 26, 194–205.

Baker, E.T., Walker, S.L., Embley, R.W., de Ronde, C.E.J., 2012. High-resolution hydrothermal mapping of Brothers Caldera, Kermadec Arc. Economic Geology 107, 1583–1593.

Bellingham, J.G., Streitlien, K., Overland, J., Rajah, S., Stein, P., Stannard, J., Kirkwood, W., Yoerger, D., 2000. An Arctic Basin observational capability using AUVs. Oceanography 13, 64–70.

Bellingham, J.G., Rajan, K., 2007. Robotics in remote and hostile environments. Science 318, 1098–1102.

Best, J.L., Kostaschuk, R.A., Peakall, J., Villard, P.V., Franklin, M., 2005. Whole flow field dynamics and velocity pulsing within natural sediment-laden underflows. Geology 33, 765–768.

Bett, B.J., 2001. UK Atlantic margin environmental survey: introduction and overview of bathyal benthic ecology. Continental Shelf Research 21, 917–956.

Bickle, M.J., Chadwick, A., Huppert, H.E., Hallworth, M.A., Lyle, S., 2007. Modelling carbon dioxide accumulation at Sleipner: implications for underground carbon storage. Earth and Planetary Science Letters 255, 164–176.

Bovio, E., Cecchi, D., Baralli, F., 2006. Autonomous underwater vehicles for scientific and naval operations. Annual Reviews in Control 30, 117–130.

Bowen, A.D., Yoerger, D.R., Taylor, C., McCabe, R., Howland, J., Gomez-Ibanez, D., Kinsey, J. C., Heintz, M., McDonald, G., Peters, D.B., Fletcher, B., Young, C., Buescher, J., Whitcomb, L.L., Martin, S.C., Webster, S.E., Jakuba, M.V., 2008. The Nereus hybrid underwater robotic vehicle for global science operations to 11,000 m depth. Proceedings of IEEE/MTS Oceans 2008, Quebec.

Brierley, A.S., Fernandes, P.G., Brandon, M.A., Armstrong, F., Millard, N.W., McPhail, S.D., Stevenson, P., Pebody, M., Perrett, J., Squires, M., Bone, D.G., Griffiths, G., 2002. Antarctic krill under sea ice: elevated abundance in a narrow band just south of ice edge. Science 295, 1890–1892.

Brito, M., Griffiths, G., Ferguson, J., Hopkin, D., Mills, R., Pedersen, R., MacNeil, E., 2012. A behavioural probabilistic risk assessment framework for managing Autonomous Underwater Vehicle deployments. Journal of Atmospheric and Oceanic Technology 29, 1689–1703.

Camilli, R., Reddy, C.M., Yoerger, D.R., Van Mooy, A.S., Jakuba, M.V., Kinsey, J.C., McIntyre, C.P., Sylva, S.P., Maloney, J.V., 2010. Tracking hydrocarbon plume transport and biodegradation at Deepwater Horizon. Science 330, 201–204.

Caratori Tontini, F., Davy, B., Dr Ronde, C.E.J., Embley, R.W., Leybourne, M., Tivey, M.A., 2012. Crustal magnetization of Brothers Volcano, New Zealand, measured by Autonomous Underwater Vehicles: geophysical expression of a submarine hydrothermal system. Economic Geology 107, 1571–1581.

Carbotte, S.M., Ryan, W.B.F., Jin, W., Cormier, M., Bergmanis, E., Sinton, J., White, S., 2003. Magmatic subsidence of the East Pacific Rise (EPR) at 18°14′S revealed through fault restoration of ridge crest bathymetry. Geochemistry, Geophysics, Geosystems 4, 1008.

Caress, D.W., Thomas, H., Kirkwood, W.J., McEwen, R., Henthorn, R., Clague, D.A., Paull, C. K., Paduan, J., 2008. High-resolution multibeam, sidescan and subbottom surveys using the MBARI AUV *D. Allan B.* In: Greene, H.G., Reynolds, J.R. (Eds.), Marine Habitat Mapping Technology for Alaska. Alaska Sea Grant College Program, University of Alaska, Fairbanks, pp. 47–69.

Caress, D.W., Clague, D.A., Paduan, J.B., Martin, J.F., Dreyer, B.M., Chadwick Jr., W.W., Denny, A., Kelley, D.S., 2012. Repeat bathymetric surveys at 1-metre resolution of lava flows erupted at Axial Seamount in April 2011. Nature Geoscience 5, 483–488.

Clague, D.A., Paduan, J.B., Caress, D.W., Thomas, H., 2011. Volcanic morphology of West Mata Volcano, NE Lau Basin, based on high-resolution bathymetry and depth changes. Geochemistry, Geophysics, Geosystems 12, QOAF03.

Coggan, R., 2012. CEND 10/12 Cruise Report. Centre for Environment, Fisheries & Aquaculture Science, Lowestoft, UK.

Connelly, D.P., Copley, J.T., Murton, B.J., Stansfield, K., Tyler, P.A., German, C.R., Van Dover, C.L., Amon, D., Furlong, M., Grindlay, N., Hayman, N., Hühnerbach, V., Judge, M., Le Bas, T., McPhail, S., Meier, A., Nakamura, K., Nye, V., Pebody, M., Pedersen, R.B., Plouviez, S., Sands, C., Searle, R.C., Stevenson, P., Taws, S., Wilcox, S., 2010. Hydrothermal vent fields and chemosynthetic biota on the world's deepest seafloor spreading centre. Nature Communications 3, 620.

Cormier, M.-H., Ryan, W.B.F., Shah, A.K., Jin, W., Bradley, A.M., Yoerger, D.R., 2003. Waxing and waning volcanism along the East Pacific Rise on a millennium time scale. Geology 31, 633–636.

Corney, R.K.T., Peakall, J., Parsons, D.R., Elliott, L., Amos, K.J., Best, J.L., Keevil, G.M., Ingham, D.B., 2006. The orientation of helical flow in curved channels. Sedimentology 53, 249–257.

Corney, R.K.T., Peakall, J., Parsons, D.R., Elliott, L., Amos, K.J., Best, J.L., Keevil, G.M., Ingham, D.B., 2008. Reply to discussion of Imran et al. on 'The orientation of helical flow in curved channels'. Sedimentology 55, 241–247.

Correa, T.B.S., Eberli, G.P., Grasmueck, M., Reed, J.K., Correa, A.M.S., 2012. Genesis and morphology of cold-water coral ridges in a unidirectional current regime. Marine Geology 326–328, 14–27.

De Santo, E., Jones, P.J.S., 2007. Offshore marine conservation policies in the North East Atlantic: emerging tensions and opportunities. Marine Policy 31, 336–347.

Deschamps, A., Tivey, M., Embley, R.W., Chadwick, W.W., 2007. Quantitative study of the deformation at Southern Explorer Ridge using high-resolution bathymetric data. Earth and Planetary Science Letters 259, 1–17.

Dinehart, R.L., Burau, J.R., 2005. Repeated surveys by acoustic Doppler current profiler for flow and sediment dynamics in a tidal river. Journal of Hydrology 314, 1–21.

Dorrell, R.M., Darby, S.E., Peakall, J., Sumner, E.J., Parsons, D.R., Wynn, R.B., 2013. Superelevation and overspill control secondary flow dynamics in submarine channels. Journal of Geophysical Research — Oceans 118, 3895–3915.

Dowdeswell, J.A., Evans, J., Mugford, R., Griffiths, G., McPhail, S., Millard, N., Stevenson, P., Brandon, M.A., Banks, C., Heywood, K.J., Price, M.R., Dodd, P.A., Jenkins, A., Nicholls, K. W., Hayes, D., Abrahamsen, E.P., Tyler, P., Bett, B., Jones, D., Wadhams, P., Wilkinson, J. P., Stansfield, K., Ackley, S., 2008. Autonomous Underwater Vehicles (AUVs) and investigations of the ice–ocean interface in Antarctic and Arctic waters. Journal of Glaciology 54, 661–672.

Dowdeswell, J.A., Evans, J., Ó Cofaigh, C., 2010. Submarine landforms and shallow acoustic stratigraphy of a 400 km-long fjord–shelf–slope transect, Kangerlussuaq margin, East Greenland. Quaternary Science Reviews 29, 3359–3369.

Dupré, S., Buffet, G., Mascle, J., Foucher, J.-P., Gauger, S., Boetius, A., Marfia, C., The AsterX AUV Team, The Quest ROV Team, The BIONIL scientific party, 2008. High-resolution mapping of large gas emitting mud volcanoes on the Egyptian continental margin (Nile Deep Sea Fan) by AUV surveys. Marine Geophysical Researches 29, 275–290.

Eddy Lee, Y.D., George, R.A., 2004. High-resolution geological AUV survey results across a portion of the Sigsbee Escarpment. AAPG Bulletin 88, 747–764.

Embley, R.W., de Ronde, C.E.J., Merle, S.G., Davy, B., Caratori Tontini, F., 2012. Detailed morphology and structure of an active submarine arc caldera: Brothers Volcano, Kermadec Arc. Economic Geology 107, 1557–1570.

Ferrini, V.L., Fornari, D.J., Shank, T.M., Kinsey, J.C., Tivey, M.A., Soule, S.A., Carbotte, S.M., Whitcomb, L.L., Yoerger, D., Howland, J., 2007. Submeter bathymetric mapping of volcanic and hydrothermal features on the East Pacific Rise crest at 9°50′N. Geochemistry, Geophysics, Geosystems 8, Q01006.

Fildani, A., Hubbard, S.M., Covault, J.A., Maier, K.L., Romans, B.W., Traer, M., Rowland, J.C., 2013. Erosion at inception of deep-sea channels. Marine and Petroleum Geology 41, 48–61.

Flood, R.D., Hiscott, R.N., Aksu, A.E., 2009. Morphology and evolution of an anastomosed channel network where saline underflow enters the Black Sea. Sedimentology 56, 807–839.

Fornari, D., Tivey, M., Schouten, H., Perfit, M., Yoerger, D., Bradley, A., Edwards, M., Haymon, R., Scheirer, D., Von Damm, K., Shank, T., Soule, A., 2004. Submarine lava flow emplacement at the East Pacific Rise 9°50′N: implications for uppermost ocean crust stratigraphy and hydrothermal fluid circulation. In: German, C.R., Lin, J., Parson, L.M. (Eds.), Mid-Ocean Ridges: hydrothermal interactions between the lithosphere and oceans. AGU Geophysical Monographs Series, 148, pp. 187–218.

Foucher, J.-P., Westbrook, G.K., Boetius, A., Ceramicola, S., Dupré, S., Mascle, J., Mienert, J., Pfannkuche, O., Pierre, C., Praeg, D., 2009. Structure and drivers of hydrocarbon seep ecosystems in the European seas: an overview from HERMES results. Oceanography 22, 92–109.

Furlong, M.E., Paxton, D., Stevenson, P., Pebody, M., McPhail, S.D., Perrett, J., 2012. Autosub Long Range: a long range deep diving AUV for ocean monitoring. 2012 IEEE/OES Autonomous Underwater Vehicles (AUV). Institute of Electrical and Electronics Engineers, Piscataway, USA, pp. 1–7.

Galerne, E., 1983. Epaulard ROV used in NOAA polymetallic sulfide research. Sea Technology 24, 40–42.

German, C.R., Bennett, S.A., Connelly, D.P., Evans, A.J., Murton, B.J., Parson, L.M., Prien, R.D., Ramirez-Llodra, E., Jakuba, M., Shank, T.M., Yoerger, D.R., Baker, E.T., Walker, S.L., Nakamura, K., 2008a. Hydrothermal activity on the southern Mid-Atlantic Ridge: tectonically- and volcanically-controlled venting at 4–5°S. Earth and Planetary Science Letters 273, 332–344.

German, C.R., Yoerger, D.R., Jakuba, M., Shank, T.M., Langmuir, C.H., Nakamura, K., 2008b. Hydrothermal exploration with the *Autonomous Benthic Explorer*. Deep-Sea Research I 55, 203–219.

Giorgio Serchi, F., Peakall, J., Ingham, D.B., Burns, A.D., 2011. A unifying computational fluid dynamics investigation on the river-like to river-reversed secondary circulation in submarine channel bends. Journal of Geophysical Research 116, C06012.

Gordon, L., 1996. Acoustic Doppler Current Profilers Principles of Operation: A Practical Primer, 2nd edition. RD Instruments Ltd, San Diego.

Graham, A.G.C., Dutrieux, P., Vaughan, D.G., Nitsche, F.O., Gyllencreutz, R., Greenwood, S.L., Larter, R.D., Jenkins, A., 2013. Seabed corrugations beneath an Antarctic ice shelf revealed by Autonomous Underwater Vehicle survey: origin and implications for the history of Pine Island Glacier. Journal of Geophysical Research 118, 1356–1366.

Grasmueck, M., Eberli, G.P., Viggiano, D.A., Correa, T., Rathwell, G., Luo, J., 2006. Autonomous Underwater Vehicle (AUV) mapping reveals coral mound distribution, morphology, and oceanography in deep water of the Straits of Florida. Geophysical Research Letters 33, L23616.

Greene, H.G., Maher, N.M., Paull, C.K., 2002. Physiography of the Monterey Bay National Marine Sanctuary and implications about continental margin development. Marine Geology 181, 55–82.

Griffiths, G., 2003. Technologies and Applications of Autonomous Underwater Vehicles. Taylor and Francis, London (360 pp.).

Haase, K.M., Koschinsky, A., Petersen, S., Devey, C.W., German, C., Lackschewitz, K.S., Melchert, B., Seifert, R., Borowski, C., Giere, O., Paulick, H., M64/1, M68/1 and M78/2 Scientific Parties, 2009. Diking, young volcanism and diffuse hydrothermal activity on the southern Mid-Atlantic Ridge: the Lilliput field at 9°33′S. Marine Geology 266, 52–64.

Hagen, P.E., Storkersen, N., Marthinsen, B.-E., Sten, G., Vestgård, K., 2008. Rapid environmental assessment with autonomous underwater vehicles — examples form HUGIN operations. Journal of Marine Systems 69, 137–145.

Hovland, M., Svensen, H., 2006. Submarine pingos: indicators of shallow gas hydrates in a pockmark at Nyegga, Norwegian Sea. Marine Geology 228, 15–23.

Huvenne, V.A.I., McPhail, S.D., Wynn, R.B., Furlong, M., Stevenson, P., 2009. Mapping giant scours in the deep ocean. EOS Transactions AGU 90, 274–275.

Huvenne, V.A.I., Tyler, P.A., Masson, D.G., Fisher, E.H., Hauton, C., Hühnerbach, V., Le Bas, T. P., Wolff, G.A., 2011a. A picture on the wall: innovative mapping reveals cold-water coral refuge in submarine canyon. PLoS One 6, e28755.

Huvenne, V.A.I., et al., 2011b. RRS *James Cook* Cruise 60, 09 May–12 June 2011. Benthic habitats and the impact of human activities in Rockall Trough, on Rockall Bank and in Hatton Basin. National Oceanography Centre Cruise Report, Southampton (133 pp.).

Jakuba, M.V., Roman, C.N., Singh, H., Murphy, C., Kunz, C., Willis, C., Sato, T., Sohn, R.A., 2008. Long-baseline acoustic navigation for under-ice autonomous underwater vehicle operations. Journal of Field Robotics 25, 861–879.

Jenkins, A., Dutrieux, P., Jacobs, S.S., McPhail, S.D., Perrett, J.R., Webb, A.T., White, D., 2010. Observations beneath Pine Island Glacier in West Antarctica and implications for its retreat. Nature Geoscience 3, 468–472.

Jerosch, K., Schlüter, M., Pesch, R., 2006. Spatial analysis of marine categorical information using indicator kriging applied to georeferenced video mosaics of the deep-sea Håkon Mosby Mud Volcano. Ecological Informatics 1, 391–406.

JNCC, 2008. Offshore Special Area of Conservation: Haig Fras SAC Selection Assessment. Joint Nature Conservation Committee, Peterborough UK (http://jncc.defra.gov.uk/PDF/HaigFras_SelectionAssessment_4.0.pdf).

Jones, D.O.B., Bett, B.J., Wynn, R.B., Masson, D.G., 2009. The use of towed camera platforms in deep-water science. Underwater Technology 28, 41–50.

Kantor, G., Fairfield, N., Jonak, D., Wettergreen, D., 2008. Experiments in navigation and mapping with a hovering AUV. Springer Tracts in Advanced Robotics 42, 115–124.

Kelley, D.S., Karson, J.A., Gretchen, L.F.-G., Yoerger, D.R., Shank, T.M., Butterfield, D.A., Hayes, J.M., Schrenk, M.O., Olson, E.J., Proskurowski, G., Jakuba, M., Bradley, A., Larson, B., Ludwig, K., Glickson, D., Buckman, K., Bradley, A.S., Brazelton, W.J., Roe, K., Elend, M.J., Delacour, A., Bernasconi, S.M., Lilley, M.D., Baross, J.A., Summons, R.E., Sylva, S.P., 2005. A serpentinite-hosted ecosystem: the Lost City hydrothermal field. Science 307, 1428–1434.

Kennish, M.J., Haag, S.M., Sakowicz, G.P., Tidd, R.A., 2004. Sidescan sonar imaging of subtidal benthic habitats in the Mullica River–Great Bay Estuarine System. Journal of Coastal Research 45, 227–240.

Khripounoff, A., Vangriesheim, A., Babonneau, N., Crassous, P., Dennielou, B., Savoye, B., 2003. Direct observation of intense turbidity current activity in the Zaire submarine valley at 4000 m water depth. Marine Geology 194, 151–158.

Kirkwood, W.J., 2007. Development of the DORADO mapping vehicle for multibeam, subbottom and sidescan science missions. Journal of Field Robotics 24, 487–495.

Kumagai, H., Tsukioka, S., Yamamoto, H., Tsuji, T., Shitashima, K., Asada, M., Yamamoto, F., Kinoshita, M., 2010. Hydrothermal plumes imaged by high-resolution sidescan sonar on a cruising AUV, Urashima. Geochemistry, Geophysics, Geosystems 11, Q12103.

Lampitt, R.S., Billett, D.S.M., Martin, A.P., 2010. The sustained observatory over the Porcupine Abyssal Plain (PAP): insights from time series observations and process studies. Deep Sea Research II 57, 1267–1271.

Larroque, C., Mercier de Lépinay, B.M., Migeon, S., 2011. Morphotectonic and fault–earthquake relationships along the northern Ligurian margin (western Mediterranean) based on high resolution, multibeam bathymetry and multichannel seismic-reflection profiles. Marine Geophysical Research 32, 163–179.

Le Bas, T., Hühnerbach, V., 1999. PRISM Processing of Remotely-sensed Imagery for Seafloor Mapping. Operators Manual Version 3.1. Southampton Oceanography Centre, UK.

Lucieer, V., Hill, N.A., Barrett, N.S., Nichol, S., 2013. Do marine substrates 'look' and 'sound' the same? Supervised classification of multibeam acoustic data using autonomous underwater vehicle images. Estuarine, Coastal and Shelf Science 117, 94–106.

Macdonald, H.A., Wynn, R.B., Huvenne, V.A.I., Peakall, J., Masson, D.G., Weaver, P.P.E., McPhail, S.D., 2011. New insights into the morphology, fill, and remarkable longevity (>0.2 m.y.) of modern deep-water erosional scours along the northeast Atlantic margin. Geosphere 7, 845–867.

Macelloni, L., Simonetti, A., Knapp, J.H., Knapp, C.C., Lutken, C.B., Lapham, L.L., 2012. Multiple resolution seismic imaging of a shallow hydrocarbon plumbing system, Woolsey Mound, Northern Gulf of Mexico. Marine and Petroleum Geology 38, 128–142.

Maier, K.L., Fildani, A., Paull, C.K., Graham, S.A., McHargue, T., Caress, D., McGann, M., 2011. The elusive character of discontinuous deep-water channels: new insights from Lucia Chica channel system, offshore California. Geology 39, 327–330.

Maier, K.L., Fildani, A., McHargue, T., Paull, C.K., Graham, S.A., Caress, D.W., 2012. Deep-water punctuated channel migration: high-resolution subsurface data from the Lucia Channel System, offshore California. Journal of Sedimentary Research 82, 1–8.

Marcon, Y., Sahling, H., Borowski, C., dos Santos Ferreira, C., Thal, J., Bohrmann, G., 2013. Megafaunal distribution and assessment of total methane and sulfide consumption by mussel beds at Menez Gwen hydrothermal vent, based on geo-referenced photomosaics. Deep-Sea Research I 75, 93–109.

Masson, D.G., Bett, B.J., Billett, D.S.M., Jacobs, C.L., Wheller, A.J., Wynn, R.B., 2003. The origin of deep-water coral-topped mounds in the northern Rockall Trough, Northeast Atlantic. Marine Geology 194, 159–180.
Mayer, L., 2006. Frontiers in seafloor mapping and visualization. Marine Geophysical Researches 27, 7–17.
McPhail, S., 2009. Autosub6000: a deep diving long range AUV. Journal of Bionic Engineering 6, 55–62.
Moline, M.A., Woodruff, D.L., Evans, N.R., 2007. Optical delineation of benthic habitat using an Autonomous Underwater Vehicle. Journal of Field Robotics 24, 461–471.
Moss, J.L., Cartwright, J., Cartwright, A., Moore, R., 2012. The spatial pattern and drainage cell characteristics of a pockmark field, Nile Deep Sea Fan. Marine and Petroleum Geology 35, 321–336.
Murton, B.J., Rouse, I.P., Millard, N.W., Flewellen, C.G., 1992. Multisensor, deep-towed instrument explores ocean floor. EOS Transactions AGU 73, 225–232.
Nakamura, K., Toki, T., Mochizuki, N., Asada, M., Ishibashi, J., Nogi, Y., Yoshikawa, S., Miyazaki, J., Okino, K., 2013. Discovery of a new hydrothermal vent based on an underwater, high-resolution geophysical survey. Deep-Sea Research I 74, 1–10.
Nakazawa, T., Ushio, M., Kondoh, M., 2011. Scale dependence of predator–prey mass ratio: determinants and applications. Advances in Ecological Research 45, 269–302.
Newman, K.R., Cormier, M.-H., Weissel, J.K., Driscoll, N.W., Kastner, M., Solomon, E.A., Robertson, G., Hill, J.C., Singh, H., Camilli, R., Eustice, R., 2008. Active methane venting observed at giant pockmarks along the U.S. mid-Atlantic shelf break. Earth and Planetary Science Letters 267, 341–352.
Nicholls, K.W., Abrahamsen, E.P., Buck, J.J.H., Dodd, P.A., Goldblatt, C., Griffiths, G., Heywood, K.J., Hughes, N.E., Kaletzky, A., Lane-Serff, G.F., McPhail, S.D., Millard, N. W., Oliver, K.I.C., Perrett, J., Price, M.R., Pudsey, C.J., Saw, K., Stansfield, S., Stott, M.J., Wadhams, P., Webb, A.T., Wilkinson, J.P., 2006. Measurements beneath an Antarctic ice shelf using an autonomous underwater vehicle. Geophysical Research Letters 33, L08612.
Normark, W.R., Paull, C.K., Caress, D.W., Ussler III, W., Sliter, R., 2009. Fine-scale relief related to Late Holocene channel shifting within the floor of the upper Redondo Fan, offshore Southern California. Sedimentology 56, 1690–1704.
Pan, C., Guo, Y., 2012. Design and simulation of high altitude air-launched automatic underwater vehicles. Applied Mechanics and Materials 128–129, 1386–1391.
Parsons, D.R., Best, J.L., Lane, S.N., Orfeo, O., Hardy, R.J., Kostaschuk, R., 2007. Form roughness and the absence of secondary flow in a large confluence–diffluence, Rio Parana, Argentina. Earth Surface Processes and Landforms 32, 155–162.
Parsons, D.R., Peakall, J., Aksu, A.E., Flood, R.D., Hiscott, R.N., Beşiktepe, S., Mouland, D., 2010. Gravity-driven flow in a submarine channel bend: direct field evidence of helical flow reversal. Geology 38, 1063–1066.
Paull, C., Ussler III, W., Maher, N., Greene, H.G., Rehder, G., Lorensen, T., Lee, H., 2002. Pockmarks off Big Sur, California. Marine Geology 181, 323–335.
Paull, C.K., Normark, W.R., Ussler III, W., Caress, D.W., Keaten, R., 2008. Association among active seafloor deformation, mound formation, and gas hydrate growth and accumulation within the seafloor of the Santa Monica Basin, offshore California. Marine Geology 250, 258–275.
Paull, C.K., Ussler III, W., Caress, D.W., Lundsten, E., Barry, J., Covault, J.A., Maier, K.L., Xu, J.P. , Augenstein, S., 2010. Origins of large crescent-shaped bedforms within the axial channel of Monterey Canyon. Geosphere 6, 755–774.
Paull, C.K., Caress, D.W., Ussler III, W., Lundsten, E., Meiner-Johnson, M., 2011. High-resolution bathymetry of the axial channels within Monterey and Soquel submarine canyons, offshore central California. Geosphere 7, 1077–1101.
Paull, C.K., Caress, D.W., Lundsten, E., Gwiazda, R., Anderson, K., McGann, M., Conrad, J., Edwards, B., Sumner, E.J., 2013. Anatomy of the La Jolla Submarine Canyon system, offshore southern California. Marine Geology 335, 16–34.
Roberts, H.H., Shedd, W., Hunt Jr., J., 2010. Dive site geology: DSV Alvin (2006) and ROV Jason II (2007) dives to the middle–lower continental slope, northern Gulf of Mexico. Deep-Sea Research II 57, 1837–1858.
Römer, M., Sahling, H., Pape, T., Bahr, A., Feseker, T., Wintersteller, P., Bohrmann, G., 2012. Geological control and magnitude of methane ebullition from a high-flux seep area in the Black Sea — the Kerch seep area. Marine Geology 319–322, 57–74.
Ruhl, H.A., et al., 2013. RRS *Discovery* Cruise 377 & 378. Autonomous ecological surveying of the abyss: understanding mesoscale spatial heterogeneity at the Porcupine Abyssal Plain. National Oceanography Centre Cruise Report No. 23, Southampton, UK (73 pp.).
Scheirer, D.S., Fornari, D.J., Humphris, S.E., Lerner, S., 2000. High-resolution seafloor mapping using the DSL-120 sonar system: Quantitative assessment of sidescan and phase-bathymetry data from the Lucky Strike Segment of the Mid-Atlantic Ridge. Marine Geophysical Researchers 21, 121–142.
Shah, A.K., Cormier, M.-H., Ryan, W.B.F., Jin, W., Sinton, J., Bergmanis, E., Carlut, J., Bradley, A., Yoerger, D., 2003. Episodic dike swarms inferred from near-bottom magnetic anomaly maps at the southern East Pacific Rise. Journal of Geophysical Research 108, 2097.
Shank, T., Fornari, D., Yoerger, D., Humpris, S., Bradley, A., Hammond, S., Lupton, J., Scheirer, D., Collier, R., Reysenbach, A.-L., Ding, K., Seyfried, W., Butterfield, D., Olson, E., Lilley, M., 2003. Deep submergence synergy: Alvin and ABE explore the Galapagos Rift at 86°W. EOS Transactions AGU 84, 425–433.
Simpson, M.R., 1986. Evaluation of a vessel-mounted acoustic Doppler current profiler for use in rivers and estuaries. Proc. 3rd Working Conference on Current Measurement. IEEE, Washington DC, pp. 106–121.
Singh, H., Armstrong, R., Gilbes, F., Eustice, R., Roman, C., Pizarro, O., Torres, J., 2004. Imaging coral I: imaging coral habitats with the SeaBED AUV. Subsurface Sensing Technologies and Applications 5, 25–42.
Statham, P.J., Connelly, D.P., German, C.R., Millard, N., McPhail, S., Pebody, M., Perrett, J., Squire, M., Stevenson, P., Webb, A., 2003. Mapping the 3D spatial distribution of dissolved manganese in coastal waters using an *in situ* analyzer and the Autonomous Underwater Vehicle *Autosub*. Underwater Technology 25, 129–134.
Statham, P.J., Connelly, D.P., German, C.R., Brand, T., Overnell, J.O., Bulukin, E., Millard, N., McPhail, S., Pebody, M., Perrett, J., Squire, M., Stevenson, P., Webb, A., 2005. Spatially complex distribution of dissolved manganese in a fjord as revealed by high-resolution in situ sensing using the Autonomous Underwater Vehicle *Autosub*. Environmental Science and Technology 39, 9440–9445.
Stevenson, P., 2011. Report on Air-launched Autonomous Underwater Vehicles. National Oceanography Centre, UK (80 pp.).
Talling, P.J., Masson, D.G., Sumner, E.J., Malgesini, G., 2012. Subaqueous sediment density flows: depositional processes and deposit types. Sedimentology 59, 1937–2003.
Talling, P.J., Paull, C.K., Piper, D.J.W., 2013. How are subaqueous sediment density flows triggered, what is their internal structure and how does it evolve? Direct observations from monitoring of active flows. Earth Science Reviews 125, 244–287.
Thomas, H., Caress, D., Conlin, D., Clague, D.A., Paduan, J., Butterfield, D., Chadwick, W., Tucker, P., 2006. Mapping AUV survey of Axial Seamount. EOS Transactions AGU 87, V23B–V0615B.
Tivey, M.A., Bradley, A., Yoerger, D., Catanach, R., Duester, A., Liberatore, S., Singh, H., 1997. Autonomous underwater vehicle maps seafloor. EOS Transactions AGU 78, 229–230.
Tivey, M.A., Johnson, H.P., Bradley, A., Yoerger, D., 1998. Thickness of a submarine laval flow determined form near-bottom magnetic field mapping by autonomous underwater vehicle. Geophysical Research Letters 25, 805–808.
Vangriesheim, A., Khripounoff, A., Crassous, P., 2009. Turbidity events observed *in situ* along the Congo submarine channel. Deep-Sea Research II 56, 2208–2222.
Vennell, R., Old, C., 2007. High-resolution observations of the intensity of secondary circulation along a curved tidal channel. Journal of Geophysical Research 112, C11008.
Wadhams, P., Wilkinson, J.P., McPhail, S.D., 2006. A new view of the underside of Arctic sea ice. Geophysical Research Letters 33, L04501.
Wagner, J.K.S., McEntee, M.H., Brothers, L.L., German, C.R., Kaiser, C.L., Yoerger, D.R., Van Dover, C.L., 2013. Cold-seep habitat mapping: high-resolution spatial characterization of the Blake Ridge Diapir seep field. Deep-Sea Research II 92, 183–188.
Wei, T., Peakall, J., Parsons, D.R., Chen, Z., Zhao, B., Best, J., 2013. Three-dimensional gravity current flow within a subaqueous bend: spatial evolution and force balance variations. Sedimentology 60, 1668–1680.
Wheeler, A.J., Bett, B.J., Masson, D.G., Mayor, D., 2005. The impact of demersal trawling on North East Atlantic deepwater coral habitats: the case of the Darwin Mounds, United Kingdom. In: Barnes, P.W., Thomas, J.P. (Eds.), Benthic habitats and the effects of fishing. American Fisheries Society Symposium, 41. Bethesda, (890 pp.).
Williams, S.B., Pizarro, O., Webster, J.M., Beaman, R.J., Mahon, I., Johnson-Roberson, M., Bridge, T.C.L., 2010. Autonomous Underwater Vehicle-assisted surveying of drowned reefs on the shelf edge of the Great Barrier Reef, Australia. Journal of Field Robotics 27, 675–697.
Wynn, R.B., Bett, B.J., Evans, A.J., Griffiths, G., Huvenne, V.A.I., Jones, A.R., Palmer, M.R., Dove, D., Howe, J.A., Boyd, T.J., MAREMAP partners, 2012. Investigating the feasibility of utilizing AUV and Glider technology for mapping and monitoring of the UK MPA network. Final Report for Defra Project MB0118. National Oceanography Centre, Southampton (244 pp.).
Xu, J.P., Barry, J.P., Paull, C.K., 2013. Small-scale turbidity currents in a big submarine canyon. Geology 41, 143–146.
Yoerger, D.R., Bradley, A.M., Walden, B.B., Singh, H., Bachmayer, R., 1998. Surveying a subsea lava flow using the Autonomous Benthic Explorer (ABE). International Journal of Systems Sciences 10, 1031–1044.
Yoerger, D.R., Bradley, A.M., Jakuba, M., German, C.R., Shank, T., Tivey, M., 2007a. Autonomous and remotely operated vehicle technology for hydrothermal vent discovery, exploration, and sampling. Oceanography 20, 152–161.
Yoerger, D.R., Jakuba, M., Bradley, A.M., 2007b. Techniques for deep sea near-bottom survey using an autonomous underwater vehicle. International Journal of Robotics Research 26, 41–54.
Yoshikawa, S., Okino, K., Asada, M., 2012. Geomorphological variations at hydrothermal sites in the southern Mariana Trough: relationship between hydrothermal activity and topographic characteristics. Marine Geology 303–306, 172–182.